PHASES OF QCD

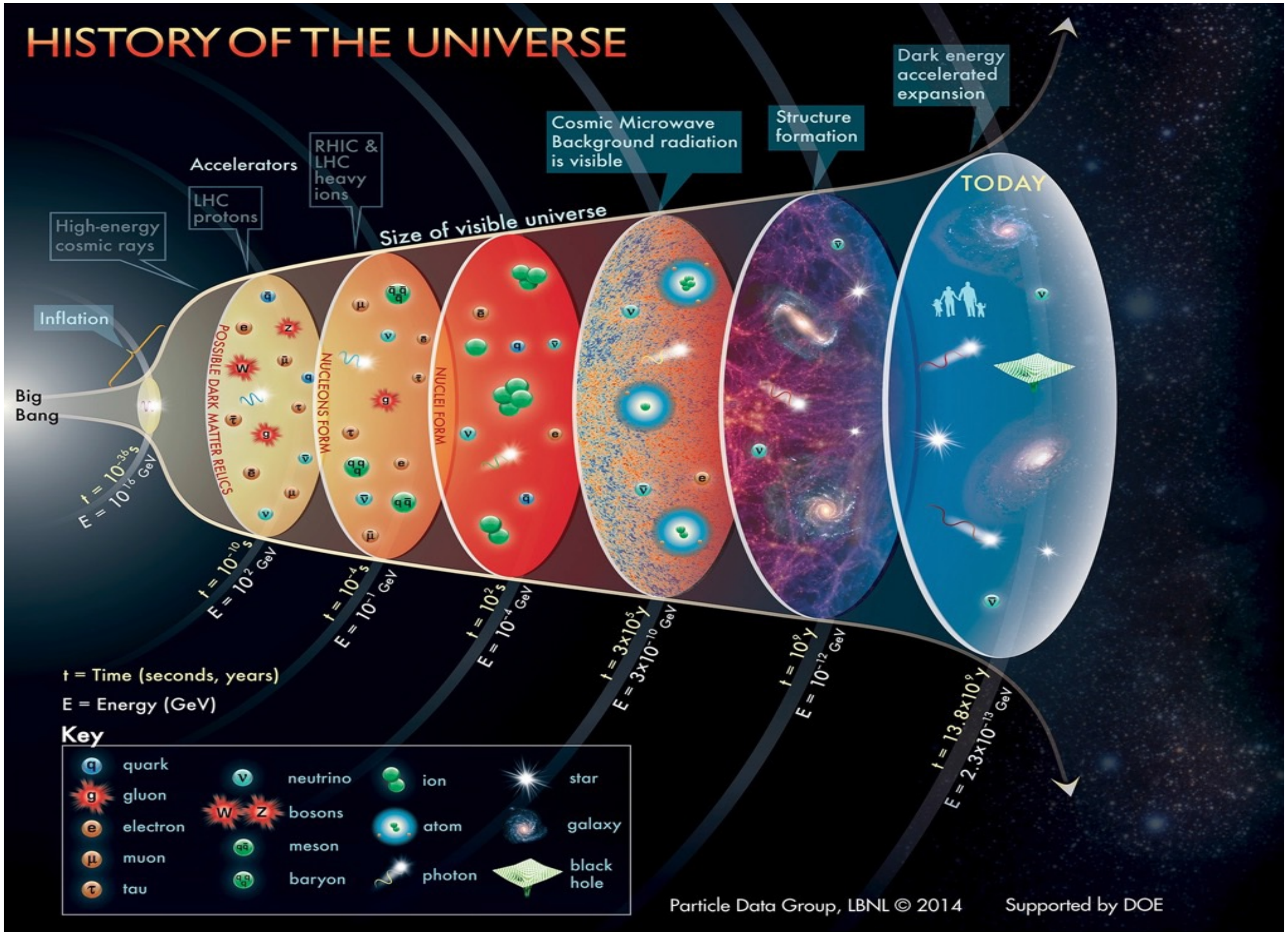

Phase Diagram for Baryonic Matter

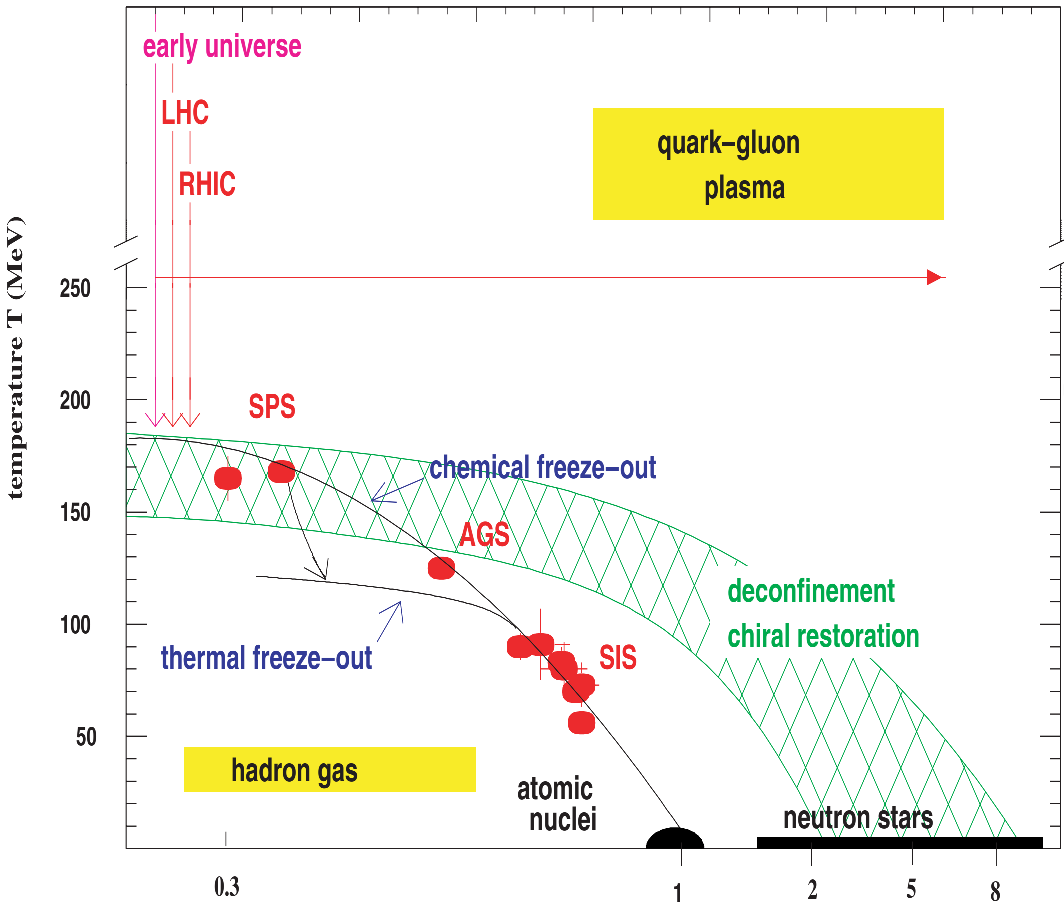

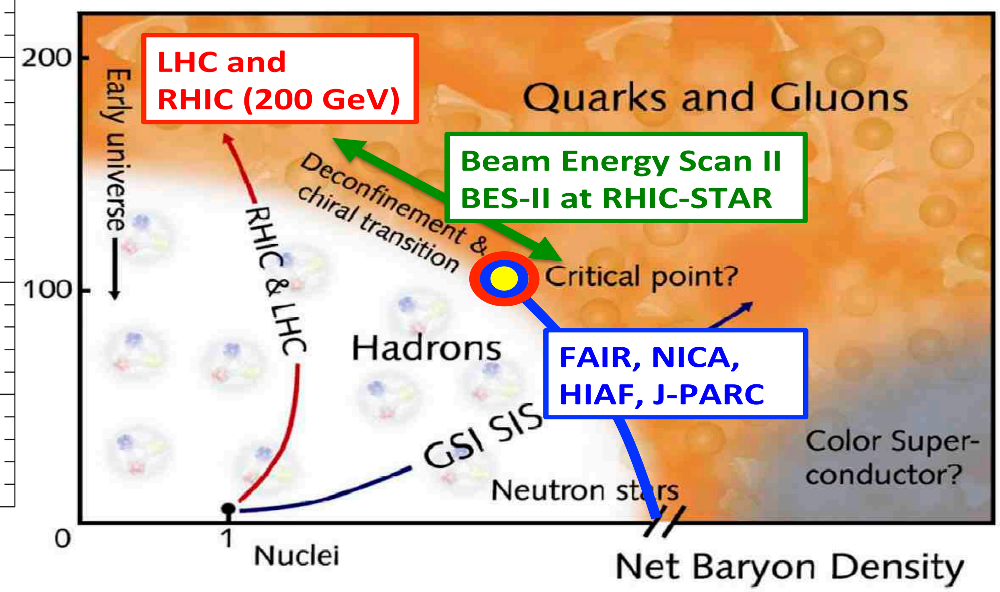

PHASES and STRUCTURES of QCD

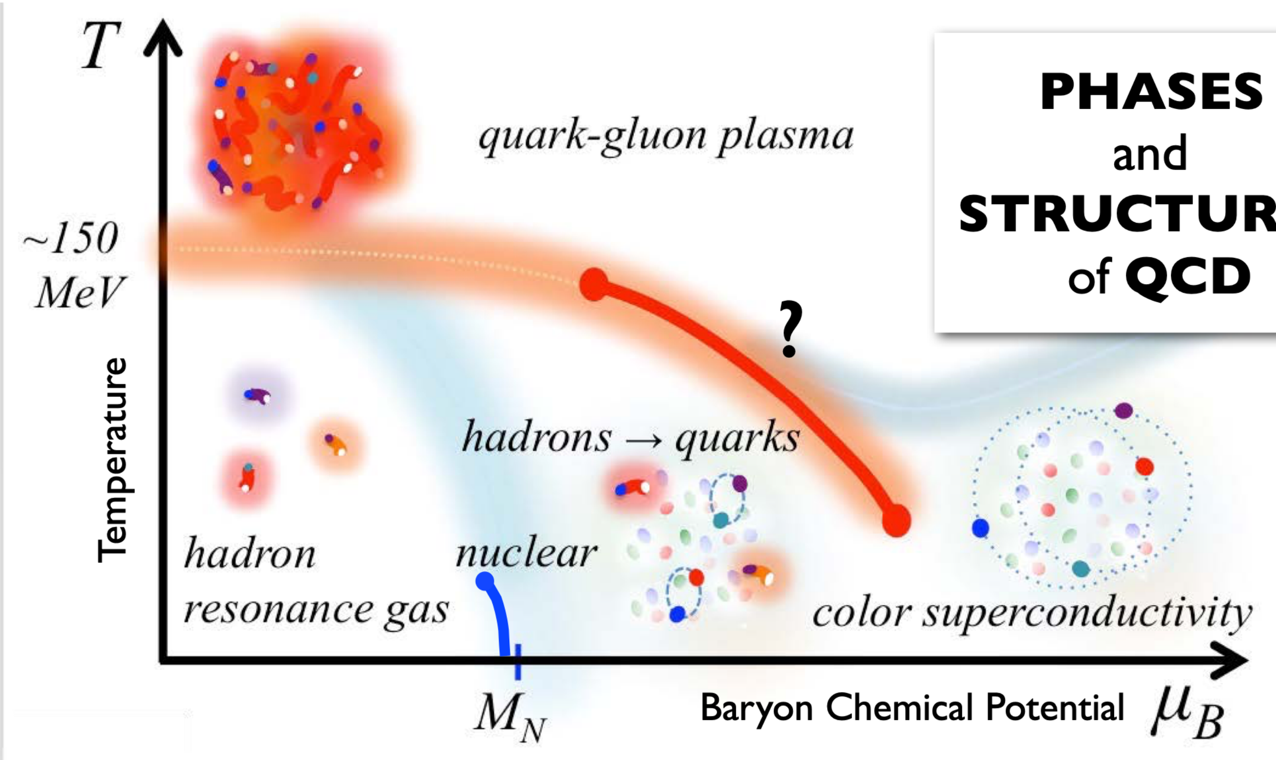

from:
G. Baym,
T. Hatsuda,
et al.

Rept. Prog. Phys.
81 (2018) 056902

Wolfram Weise
Technische Universität München
PHYSIK DEPARTMENT

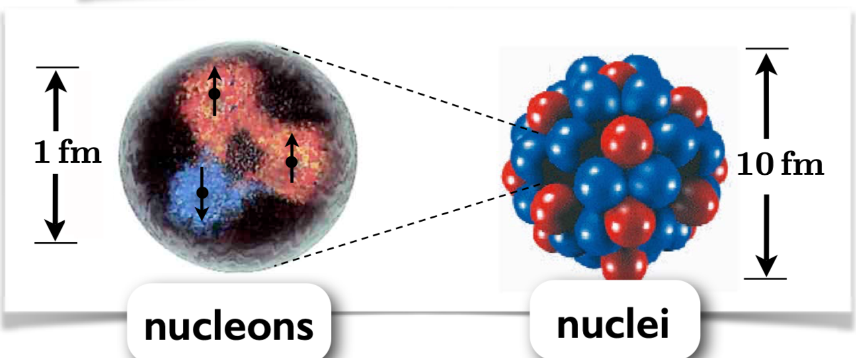

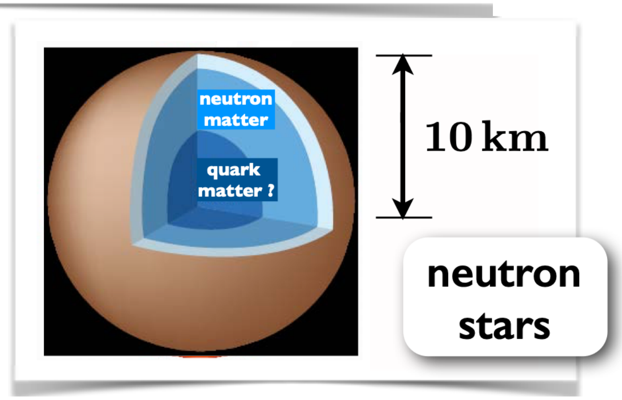

Part I: Hot baryonic matter (HI collisions)

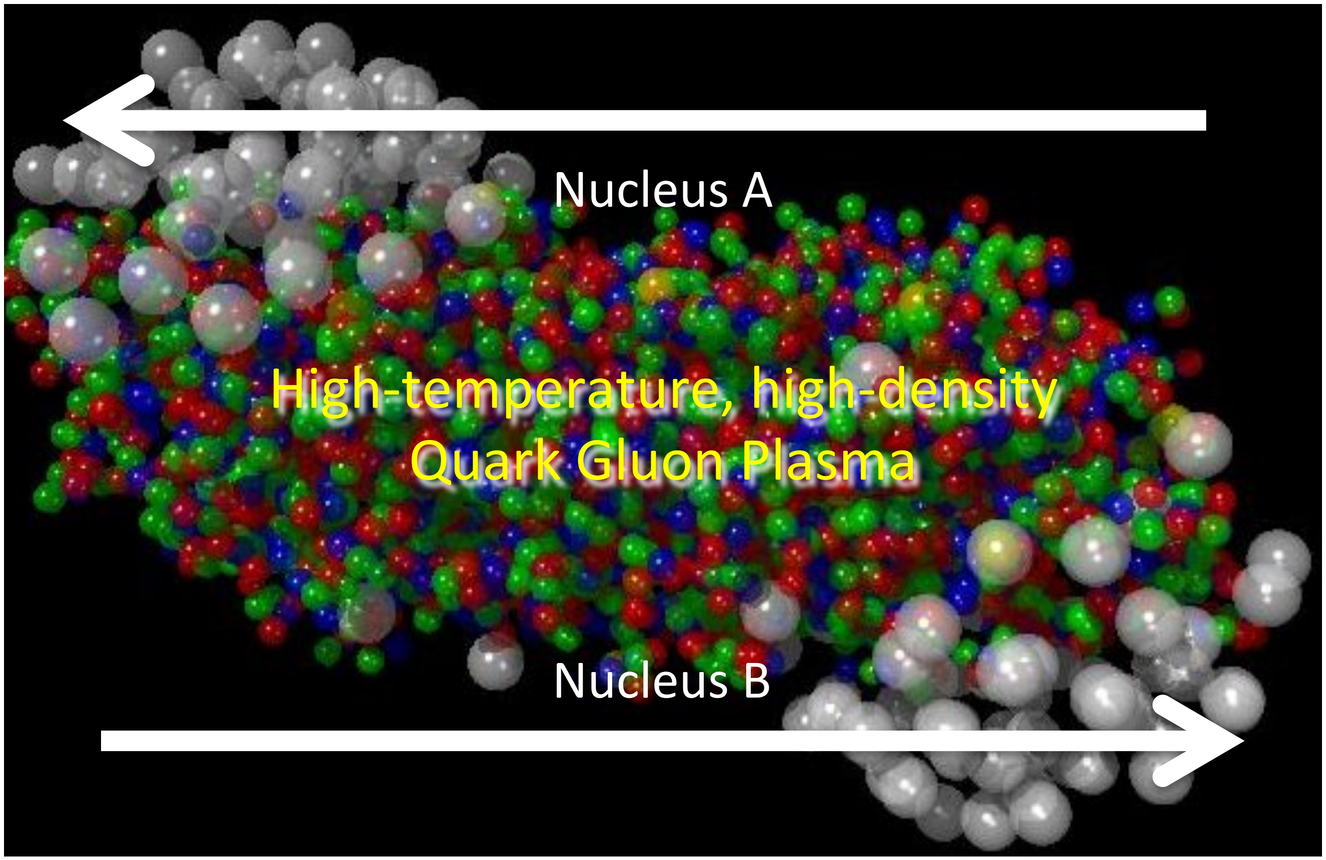

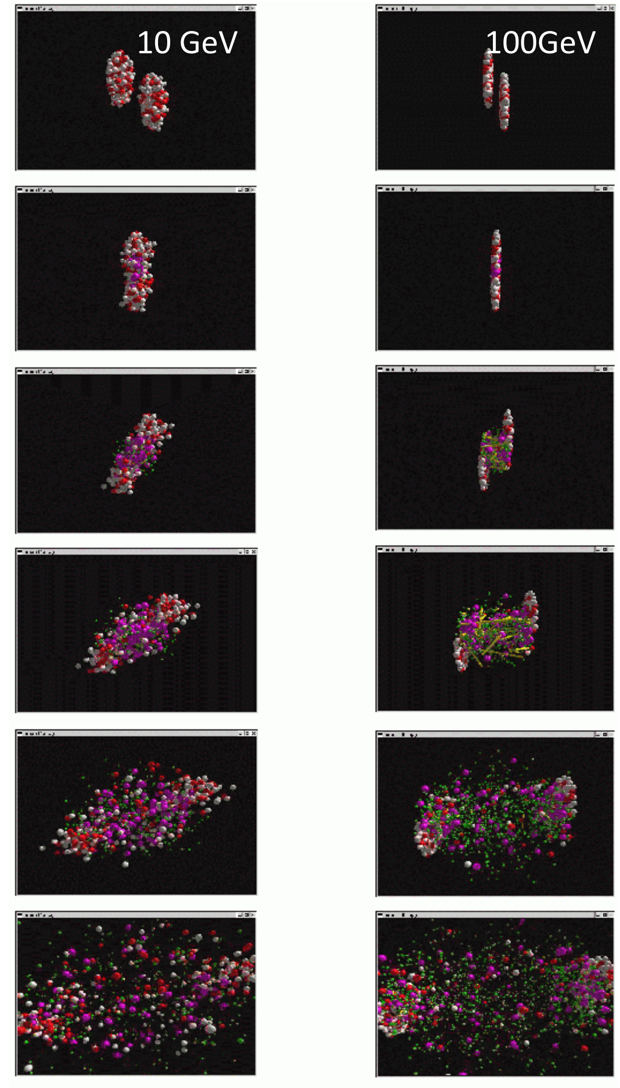

ShinIchi Esumi, Univ. of Tsukuba, TCHoU

“Standard Model” of HI Collisions

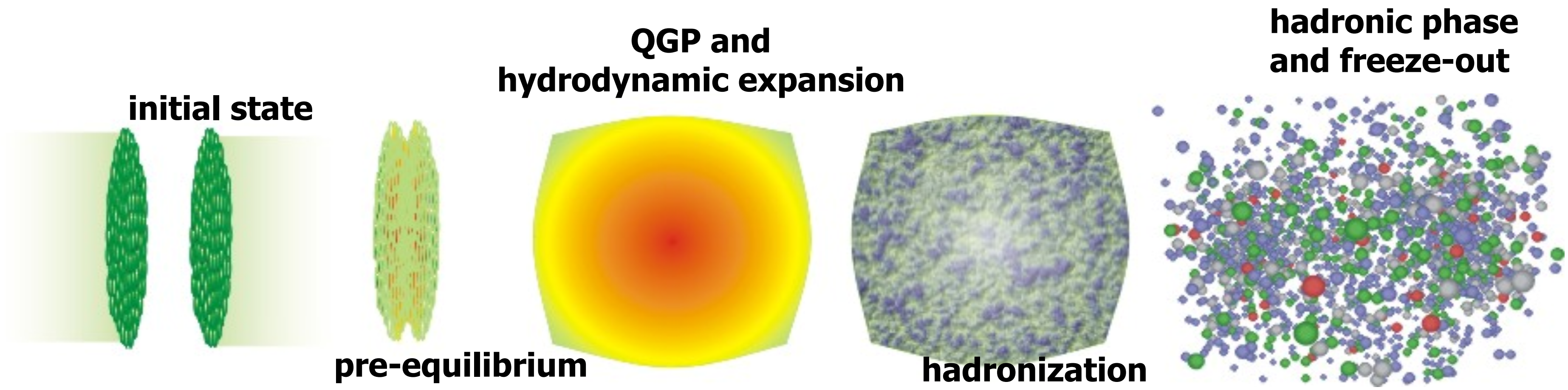

CGC | “Glasma” | Hydrodynamics | Hadronic gas

fast moving nuclei

nuclei collide

expanding & cooling QGP

hadrons re-formed

observed in experiments

High-energy heavy-ion accelerators :
AGS/RHIC at BNL
SPS/LHC at CERN
From few GeV to few TeV

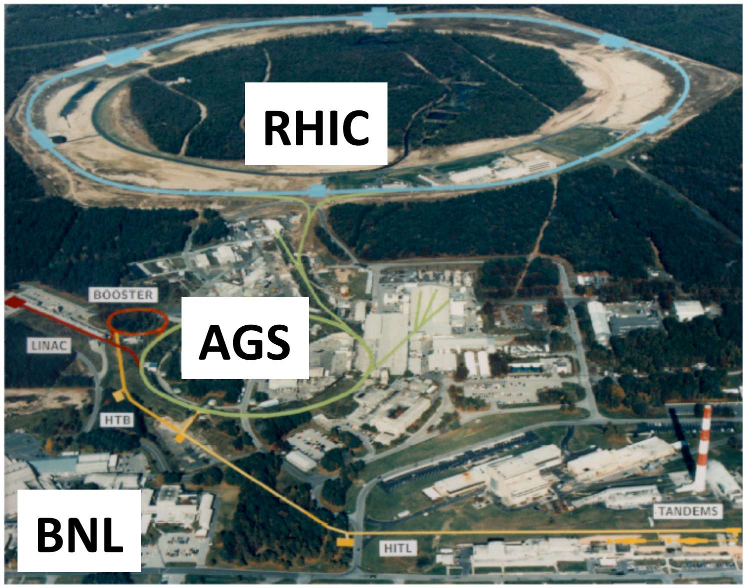

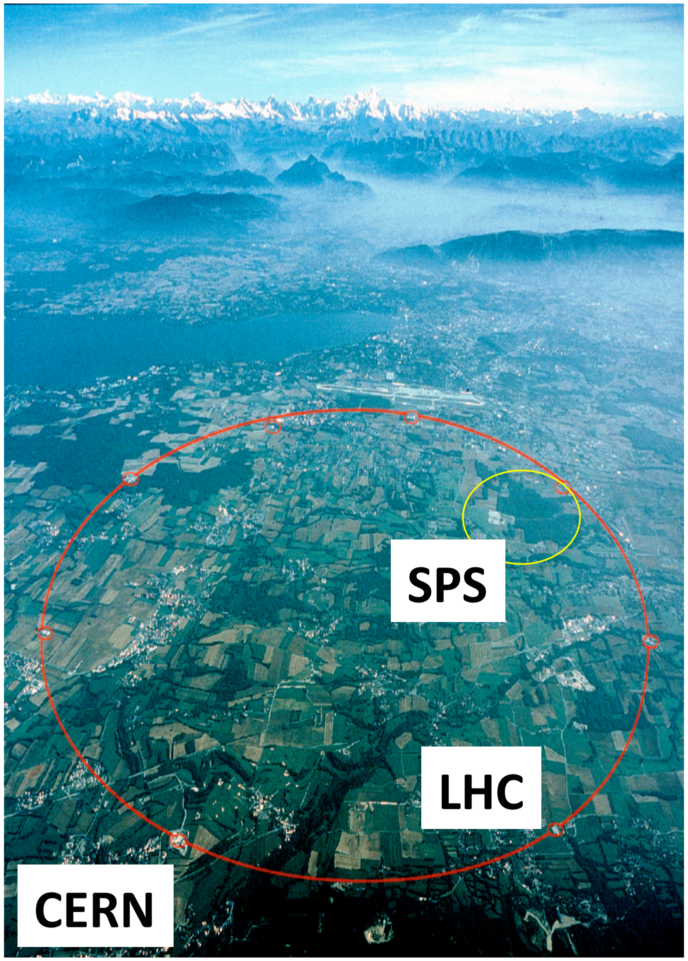

Experiments at RHIC and LHC

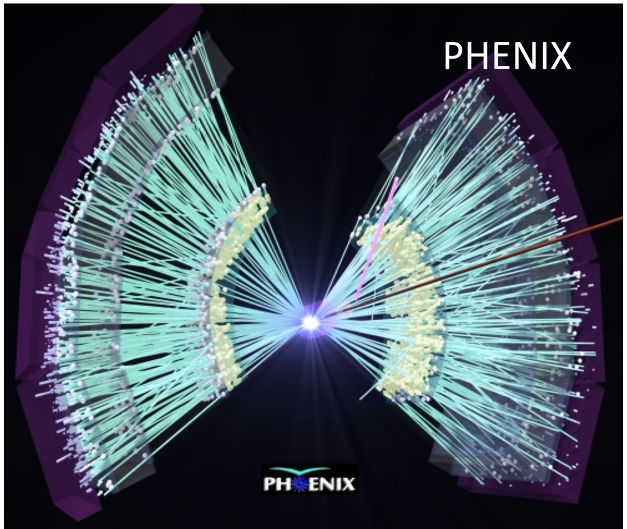

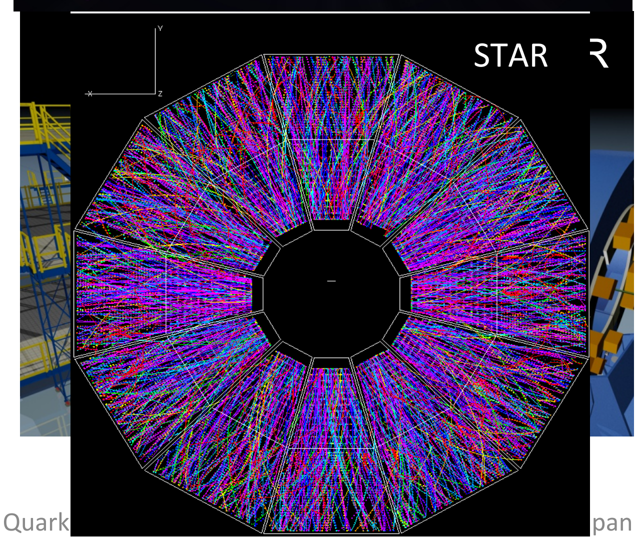

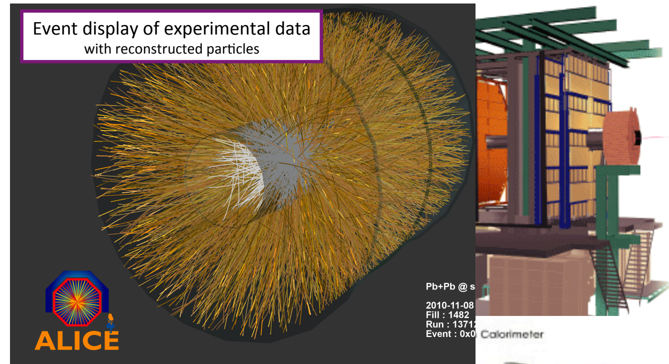

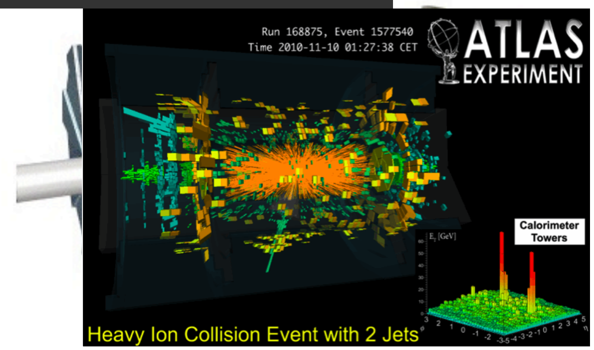

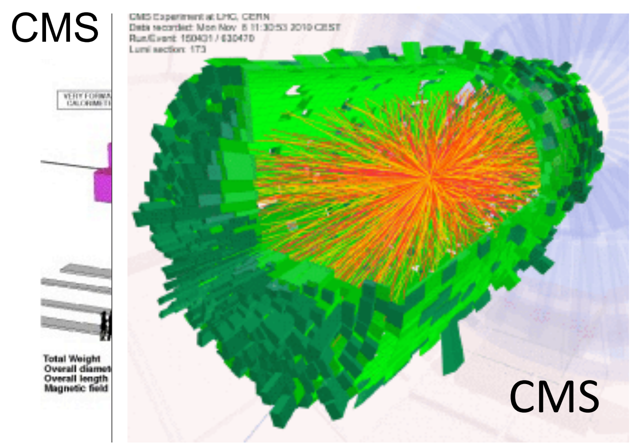

J/ψ suppression and regeneration at LHC

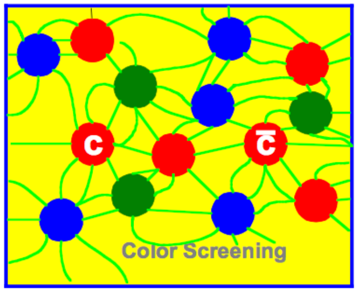

arXiv:1805.04383

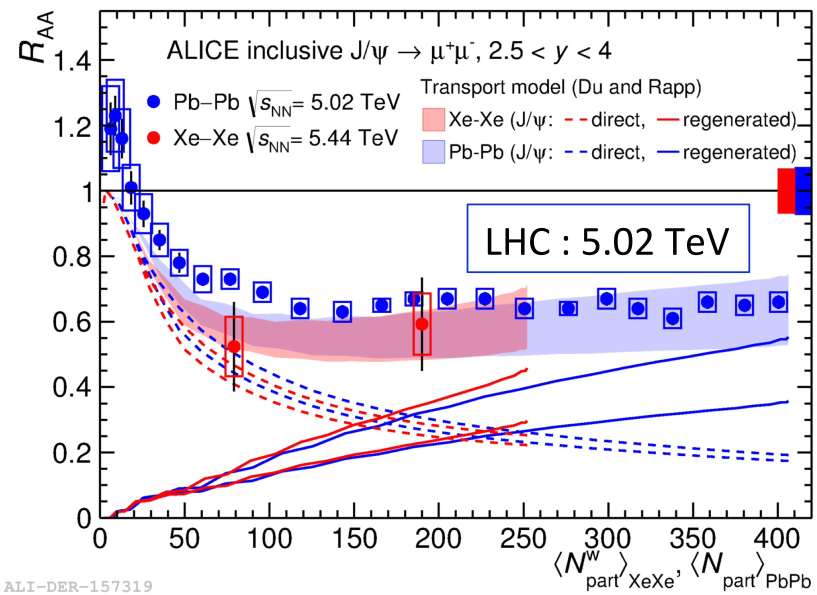

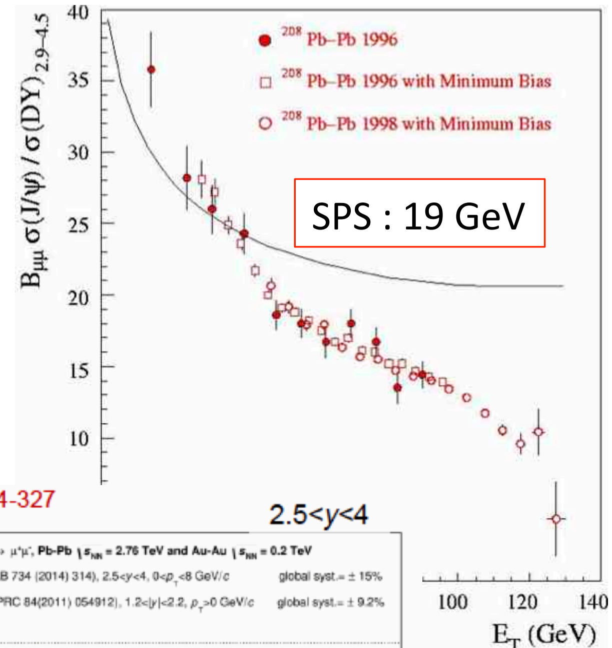

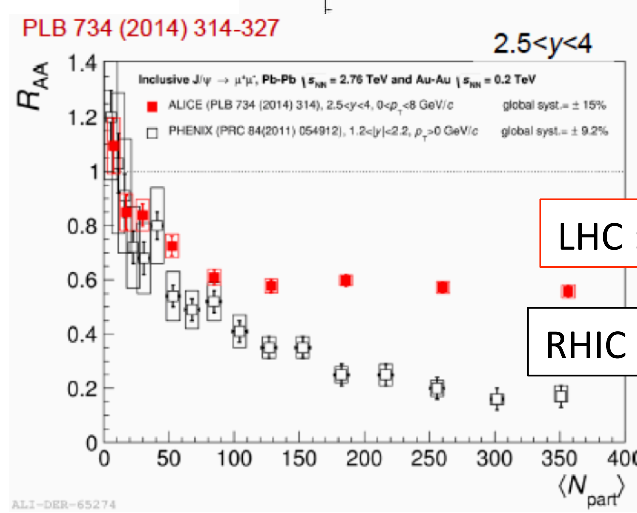

----- Suppression of initial J/ψ

——— Regenerated J/ψ

consistent with charm coalescence scenario
confirmed by J/ψ and charm flow (v_2)

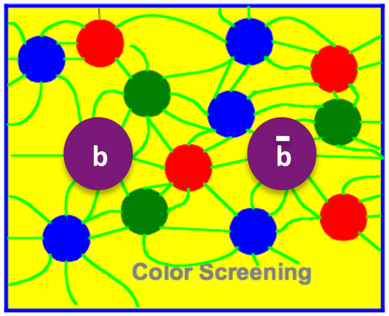

ϒ (Upsilon) suppression at LHC

--- more likely from color screening (like J/ψ at SPS/RHIC) ---

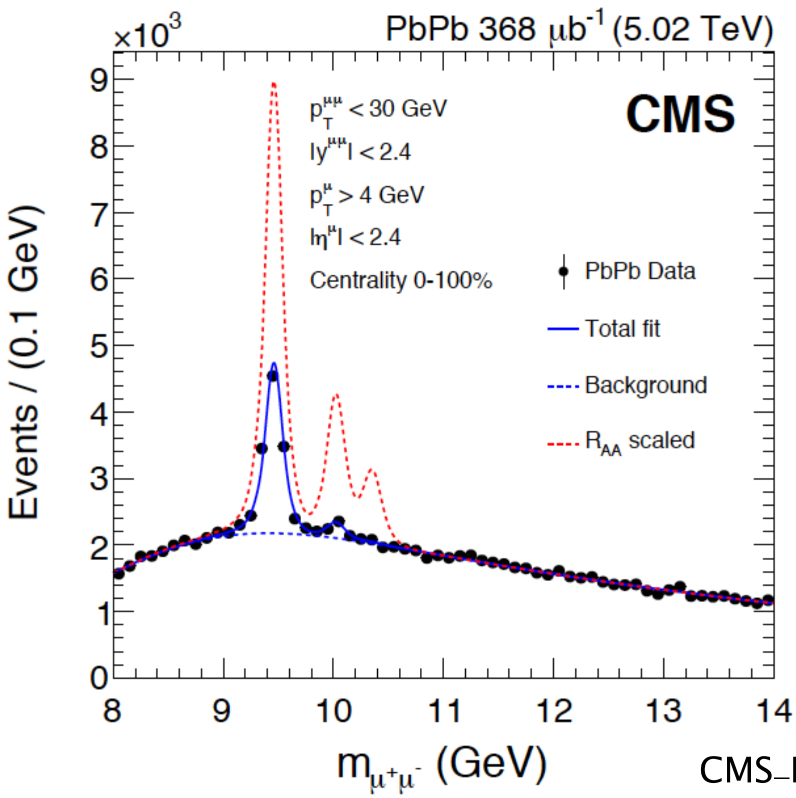

CMS_HIN_16_023

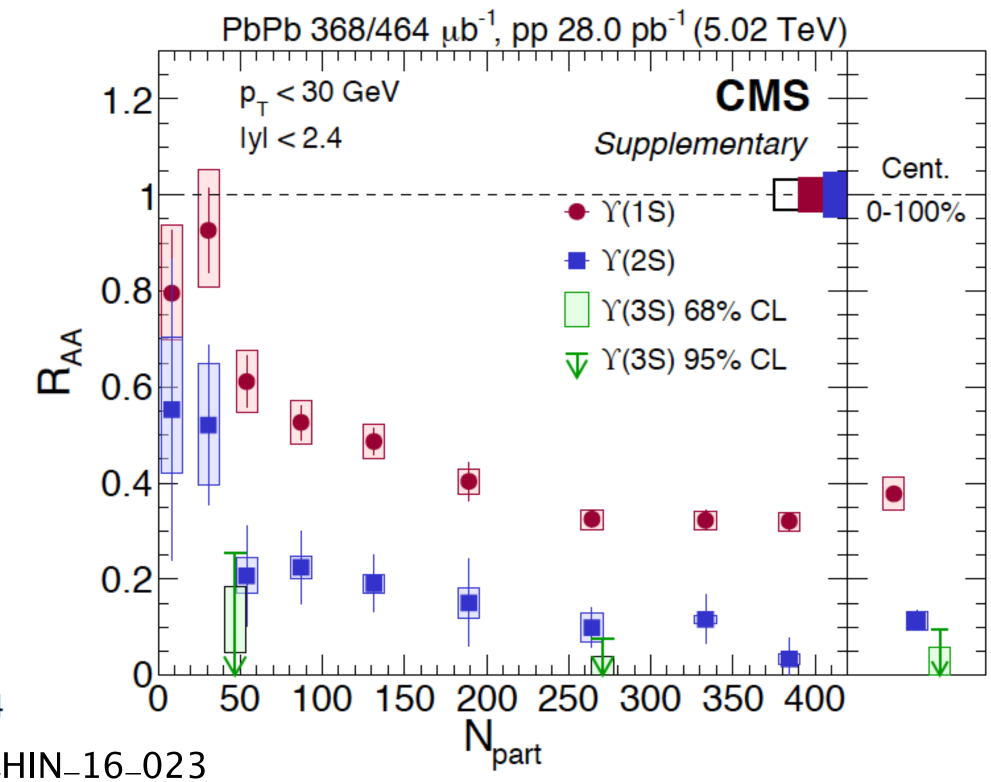

Jet quenching (high p_T suppression)

--- partonic energy-loss ---

--- penetration of direct photon ---

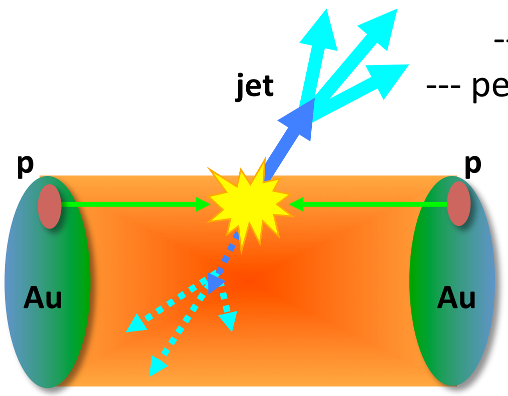

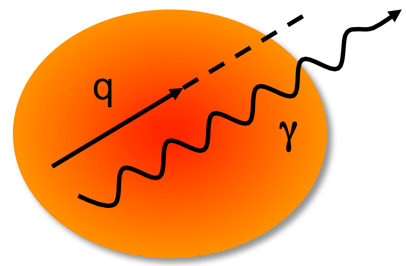

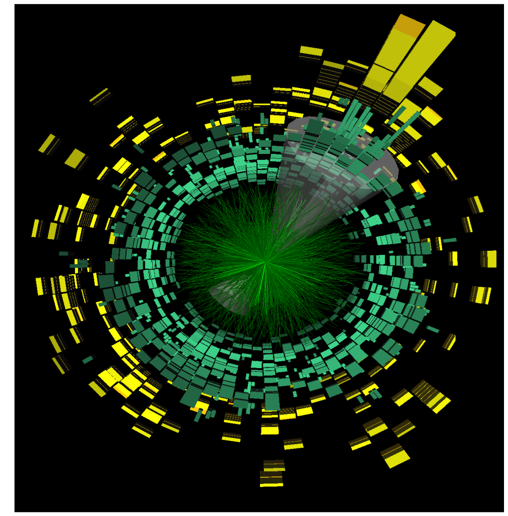

Figure 2.12: A single LHC heavy-ion collision with one high energy jet (upper right) and no apparent partner jet—because it has been quenched by the QGP produced in the collision.

PRL 91 (2003) 072304

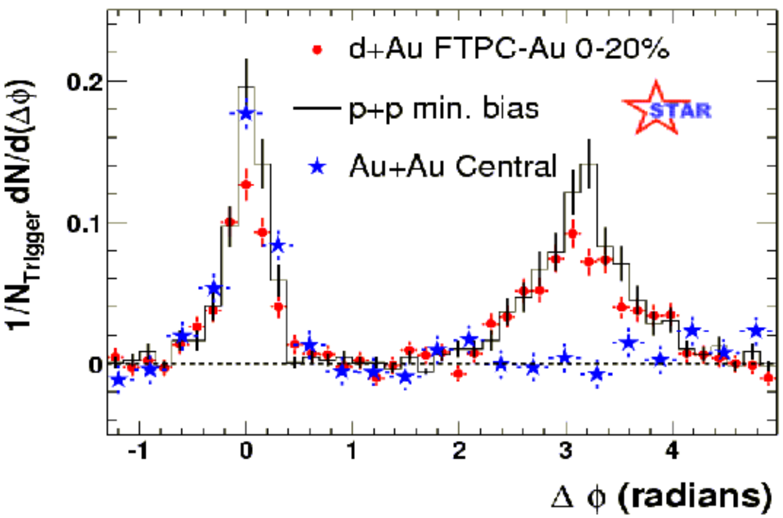

PRL109 (2012) 152302, PRC 87 (2013) 034911

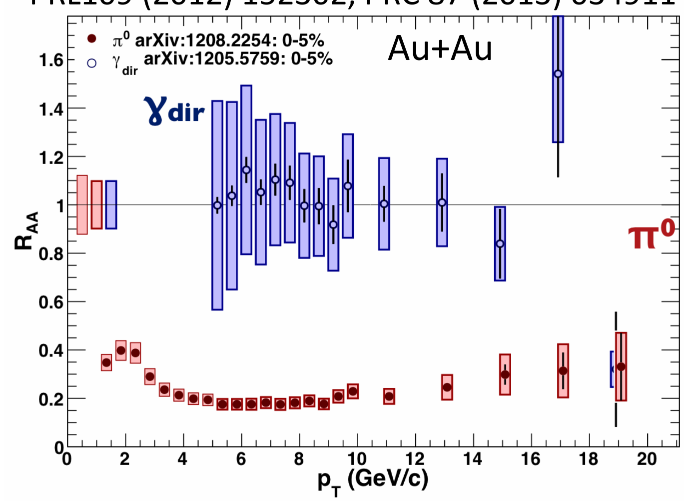

A huge surprise at RHIC was the discovery that QGP is a liquid, a result then confirmed at the LHC. And not just any liquid: it flows with the lowest specific viscosity (characterized in terms of the ratio of shear viscosity to entropy density η/s) of any liquid known, for example, more than ten times smaller than that of water. Over the past five years nuclear physicists have begun to quantify just how perfect the QGP liquid is by virtue of enormous progress on two primary fronts.

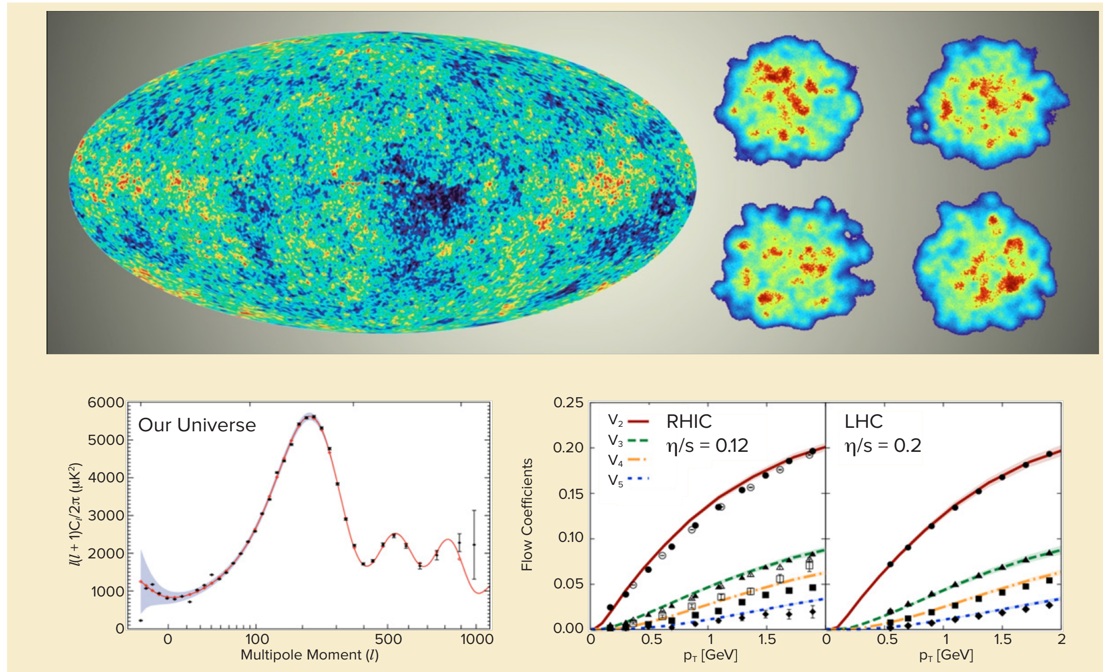

the η/s of QGP is very close to a fundamental quantum limiting value deduced for the extreme hypothetical case when the quarks and gluons have infinitely strong interactions.

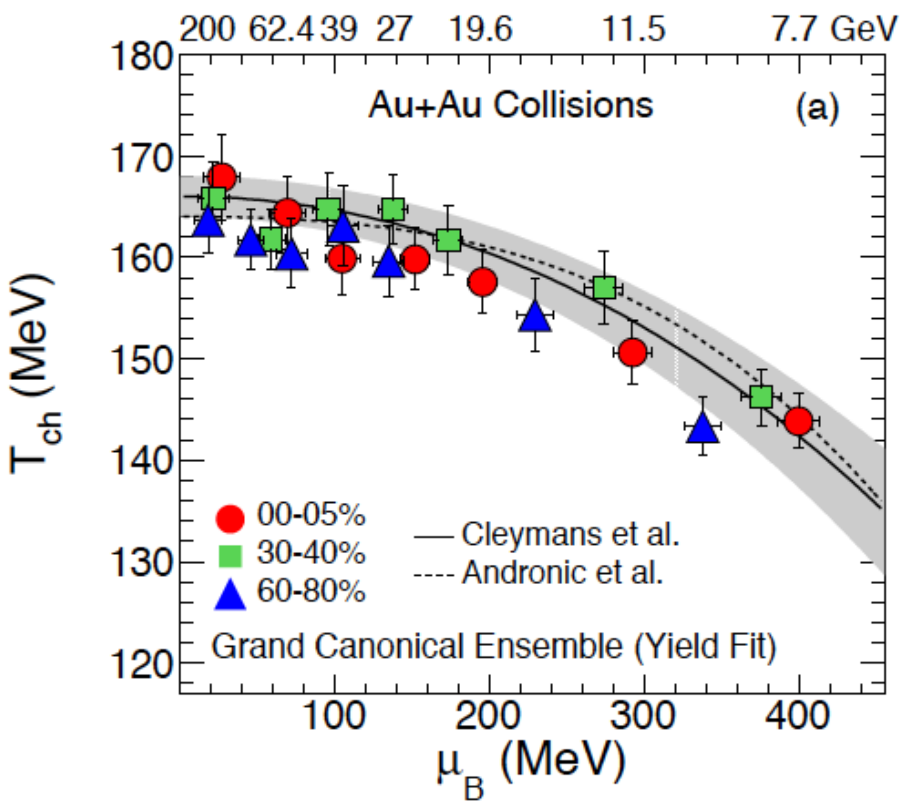

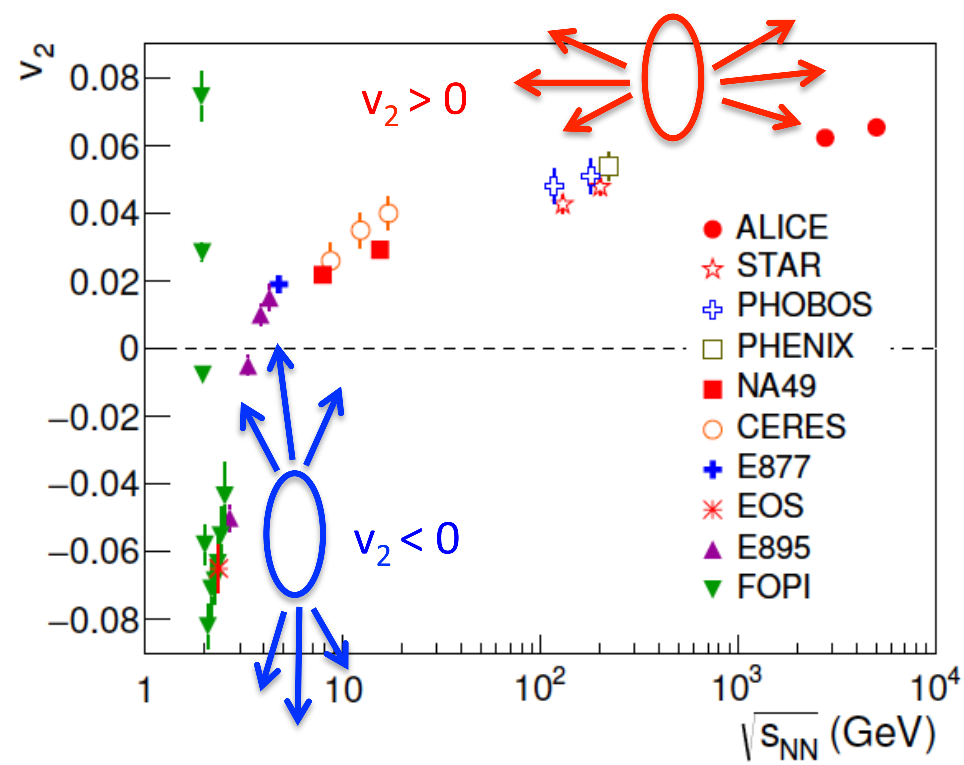

Phys. Rev. Lett. 118 (2017) 212301

Baryon density increases with decreasing beam energy.

v_2 evolution with beam energy and quark coalescence

Flow in small systems

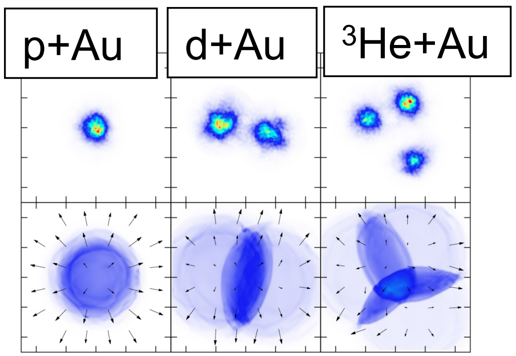

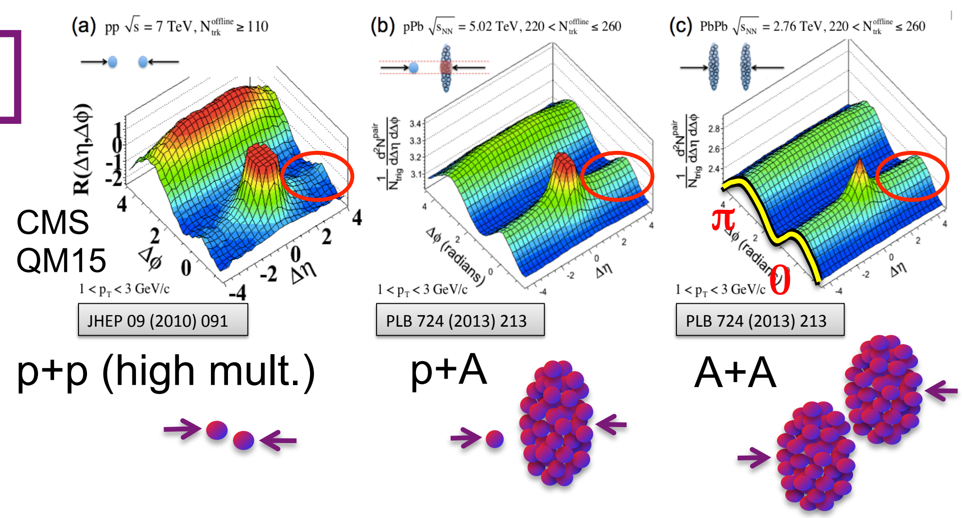

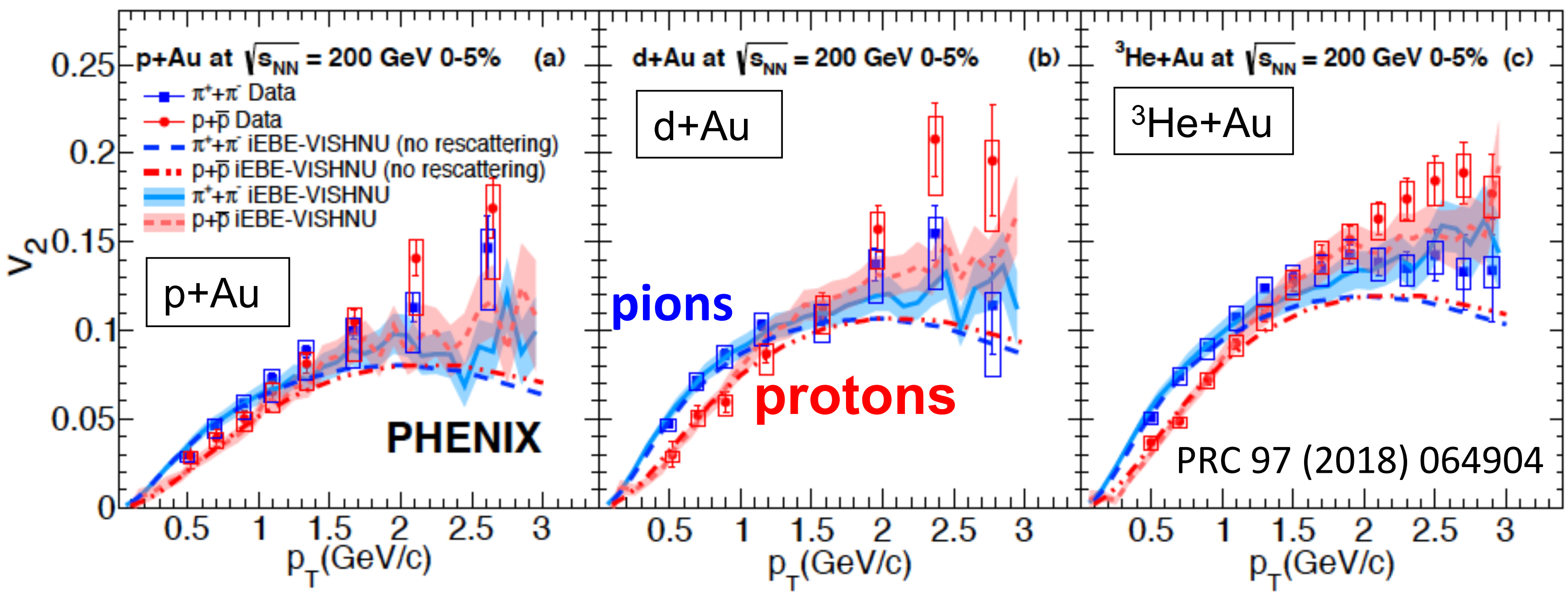

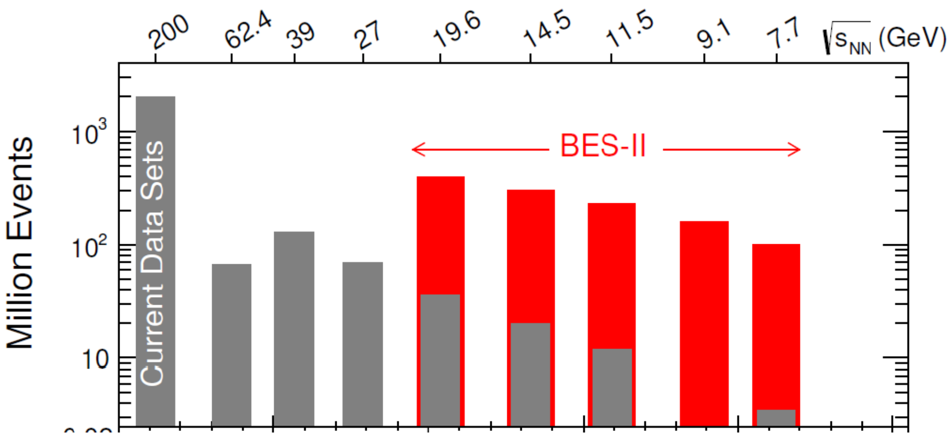

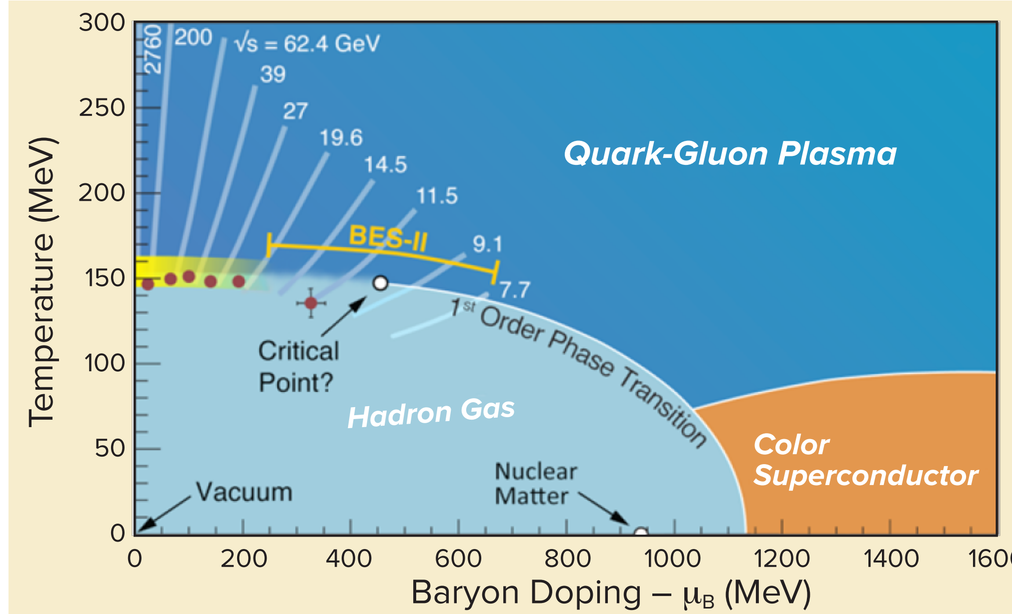

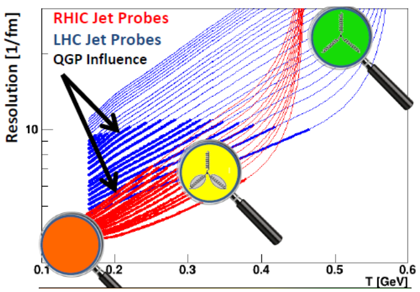

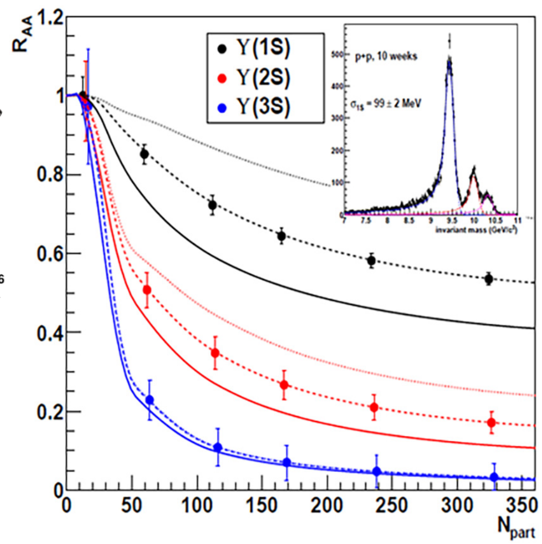

Figure 2.11: *The projected sPHENIX mass separation of the three upsilon states (in the inset) and the projected accuracy of measuring their nuclear suppression in collisions with varying impact parameters. Three sets of theory curves show the melting dependence on the degree of fluid perfection.*

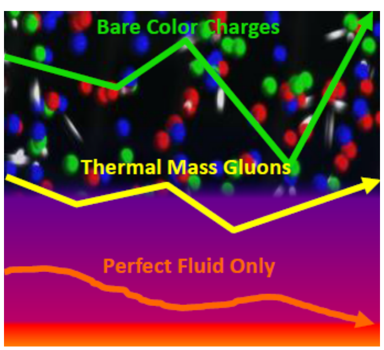

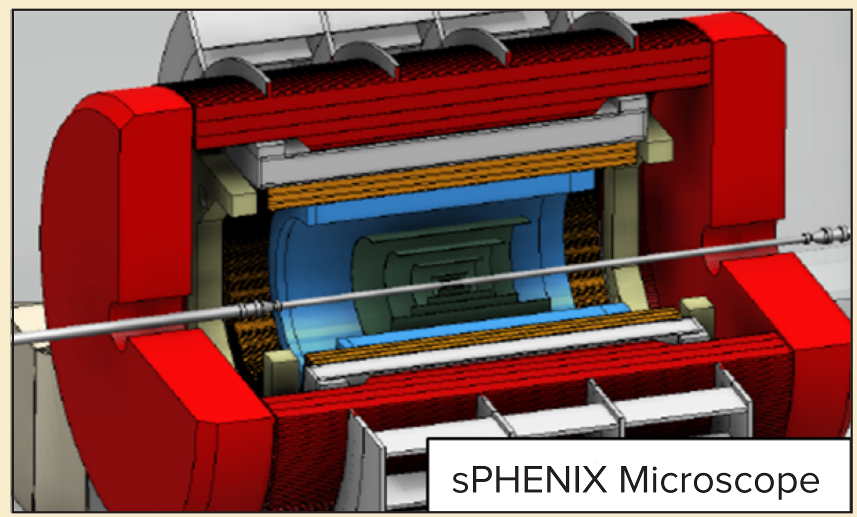

Part II: Cold baryonic matter (High Density)

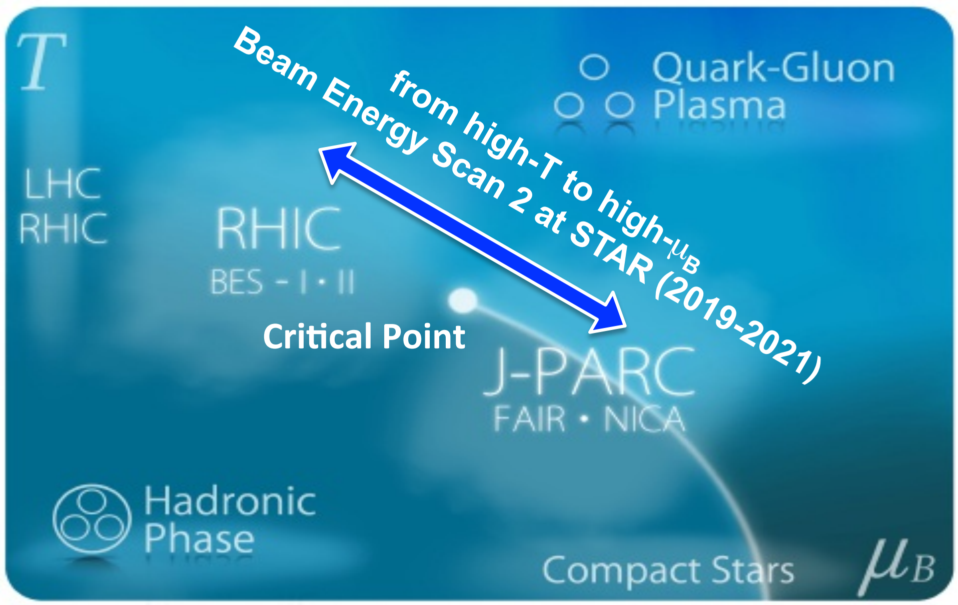

Chiral Soliton Model of the Nucleon:

Spontaneously broken chiral symmetry + localisation (confinement)

- **NUCLEON : compact valence quark core + mesonic cloud**

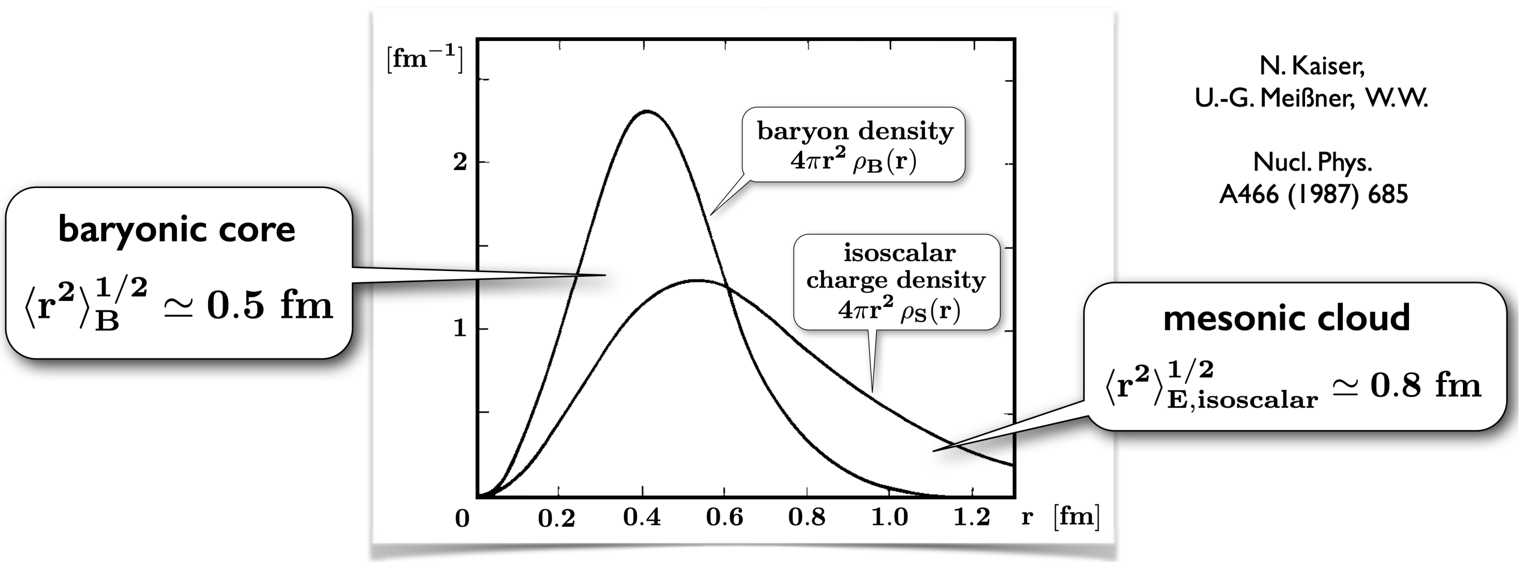

N. Kaiser, U.-G. Meißner, W.W.

Nucl. Phys. A466 (1987) 685

- Significant difference of scales between **compact baryonic core** and (multi-)**pion cloud**

Transverse distributions of **quarks** in the **proton**

Deeply Virtual Compton Scattering @ JLab

R. Dupré, M. Guidal, M. Vanderhaeghen
Phys. Rev. D95 (2017) 011501

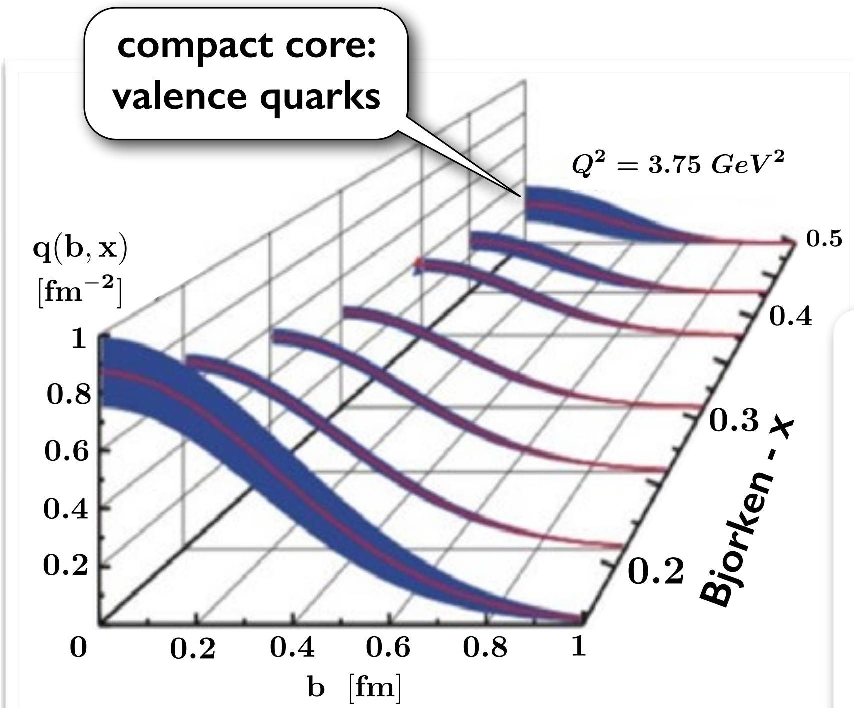

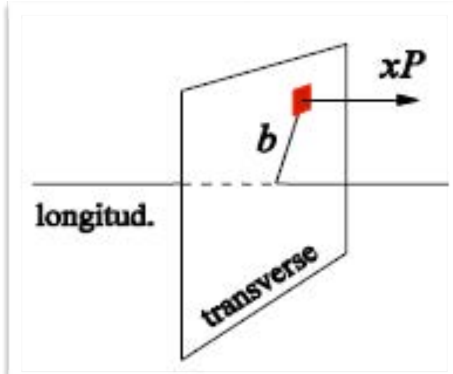

$$\langle b^2 \rangle \simeq 0.16\,\mathrm{fm}^2 \cdot \ln(1/x_B)$$

- **Valence quark region:**

$$\frac{1}{3} < x_B < \frac{1}{2}$$

- **Core size:**

$$R_{core} = \sqrt{\frac{3}{2}\langle b^2 \rangle} \sim 0.4 - 0.5\ \mathrm{fm}$$

Densities and **Distance Scales** in **Baryonic Matter**

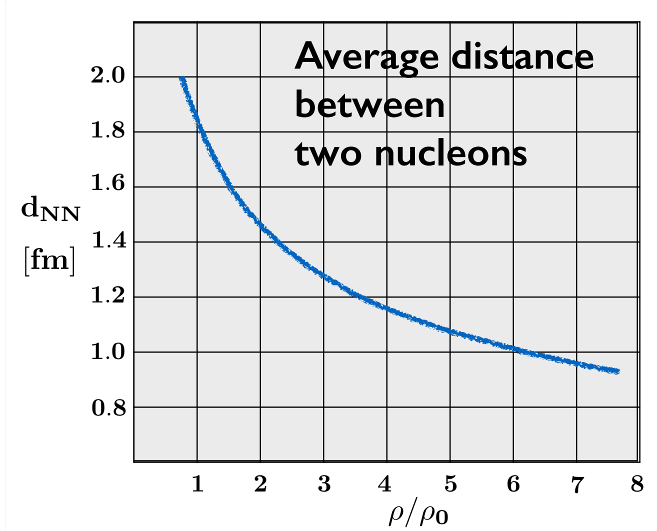

normal nuclear matter

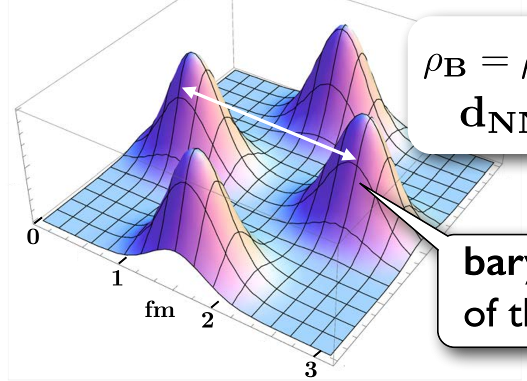

$\rho_B = \rho_0 = 0.16\ \mathrm{fm}^{-3}$

$d_{NN} \simeq 1.8\ \mathrm{fm}$

baryonic core of the nucleon

neutron star core matter

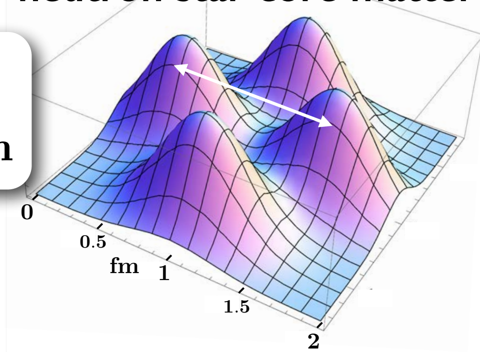

$\rho_B \sim 5\,\rho_0$

$d_{NN} \sim 1\ \mathrm{fm}$

- (Multi-)pion fields in space between baryonic sources (ChEFT)
- Quark cores of nucleons overlap (percolate) at baryon densities $\rho_B > 5\,\rho_0$

Hadron spectrum and QCD condensates

- Dynamical mass generation due to spontaneous symmetry breaking:
  - Hadron mass: breaking of scale invariance (trace anomaly)
  - Parity splitting, Goldstone modes: breaking of χ symmetry
- Is quantum entanglement the origin of phase space "driven" particle yields?

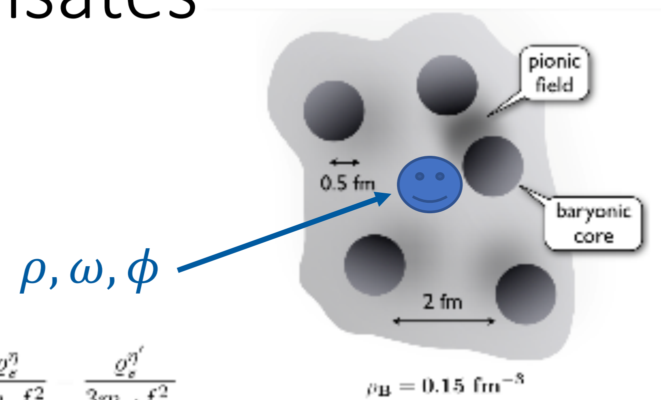

W. Weise, QNP2018

lQCD – WB group; arXiv:1005.3508

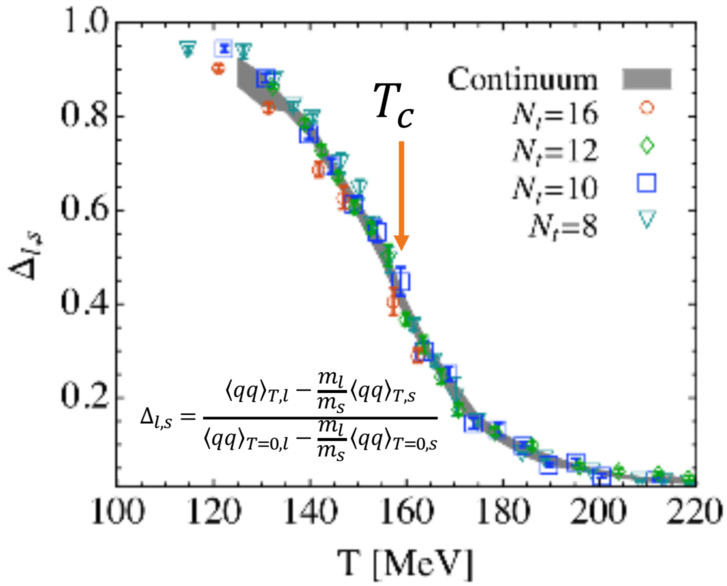

$$\frac{\langle\bar qq\rangle_T}{\langle\bar qq\rangle_0} = 1 - \frac{\varrho_s^\pi}{2m_\pi f_\pi^2} - \frac{\varrho_s^K}{4m_K f_K^2} - \frac{\varrho_s^\eta}{6m_\eta f_\eta^2} - \frac{\varrho_s^{\eta'}}{3m_{\eta'} f_{\eta'}^2} - \sum_B \frac{\sigma_B}{f_\pi^2 m_\pi^2}\varrho_s^B - \sum_M \frac{\sigma_M}{f_\pi^2 m_\pi^2}\varrho_s^M - \alpha T^{10}\,.$$

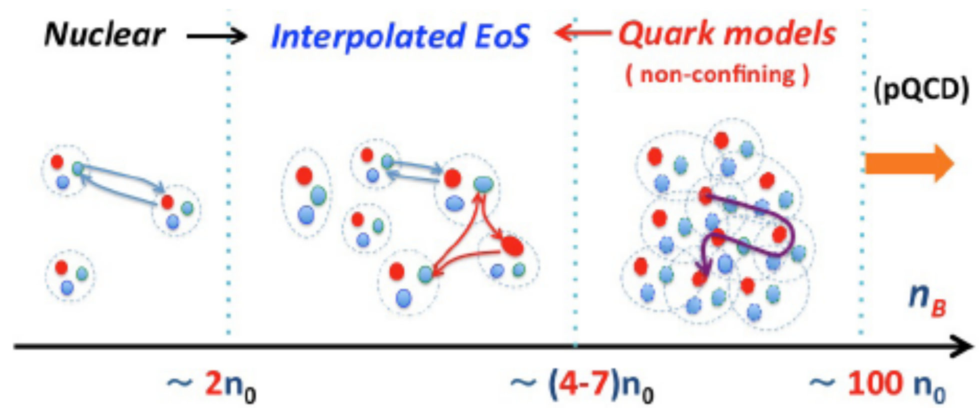

G. Baym, QNP2018

NUCLEAR FORCES from LATTICE QCD

NN Central Potential (S = 0, I = 1)
deduced from LQCD two-nucleon (6-quark) correlation function

previously:
unphysically large
u- and d-quark
masses

…but :
stable 0.5 Fermi
repulsive core

S. Aoki, T. Hatsuda, N. Ishii
Prog. Theor. Phys. 123 (2010) 89

S. Aoki
Eur. Phys. J. A49 (2013) 81

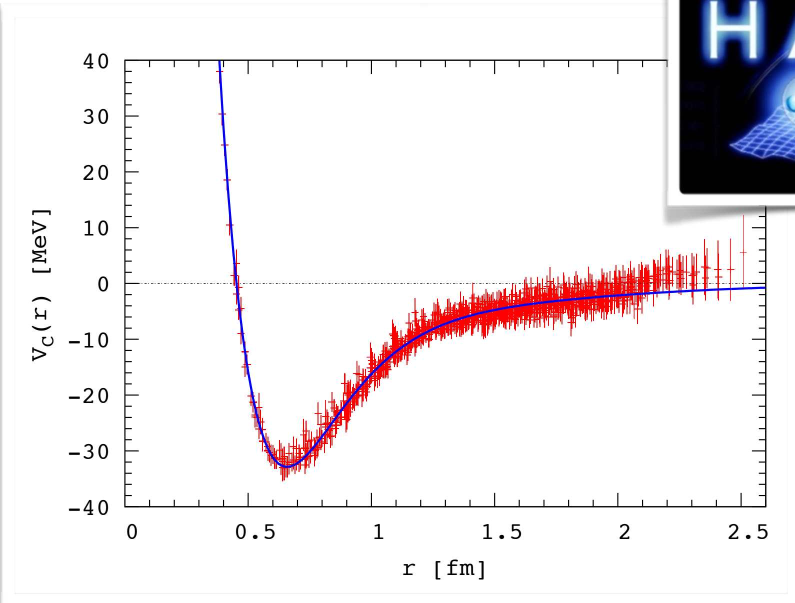

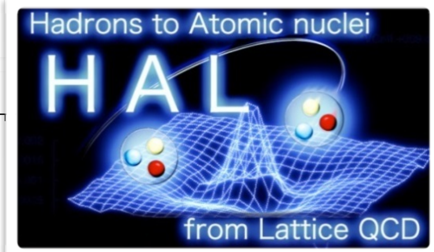

now:

towards
**physical
quark
masses**

- **Compression of baryonic matter is energetically expensive**

Heavy-ion collisions and neutron star merger

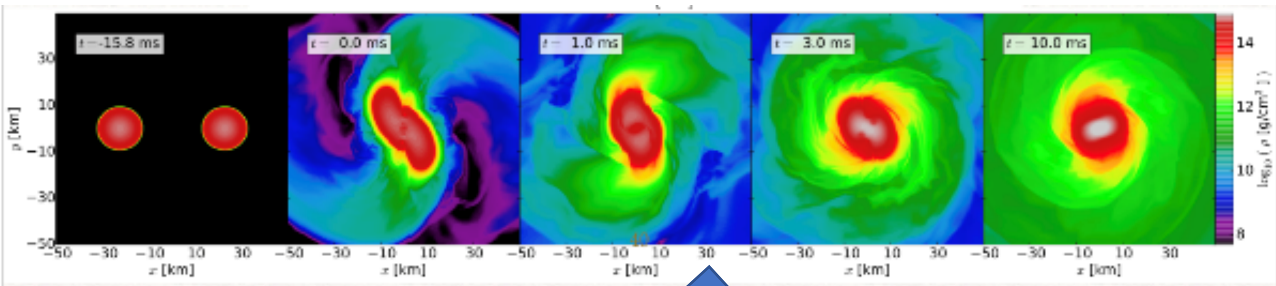

M. Hanauske, J. Steinheimer (priv. com.)
L. Rezzolla et al. arXiv:1807.03684

Gravitantional wave signal can probe the dense EOS during "ring down" if frequencies in kHZ range are detected.

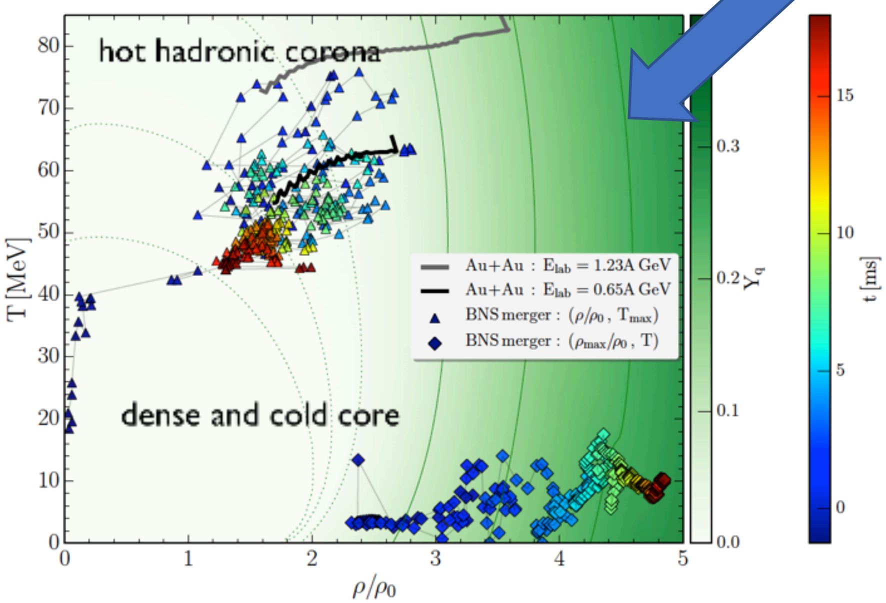

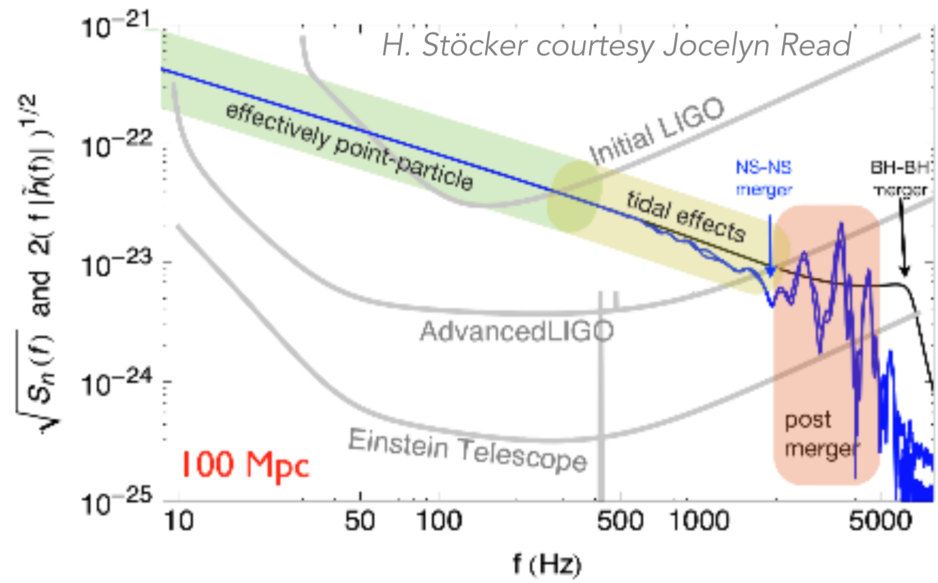

Vector mesons in cold matter

- Ideal probe to monitor possible mass shifts
- Low relative momentum to medium needed to increase sensitivity

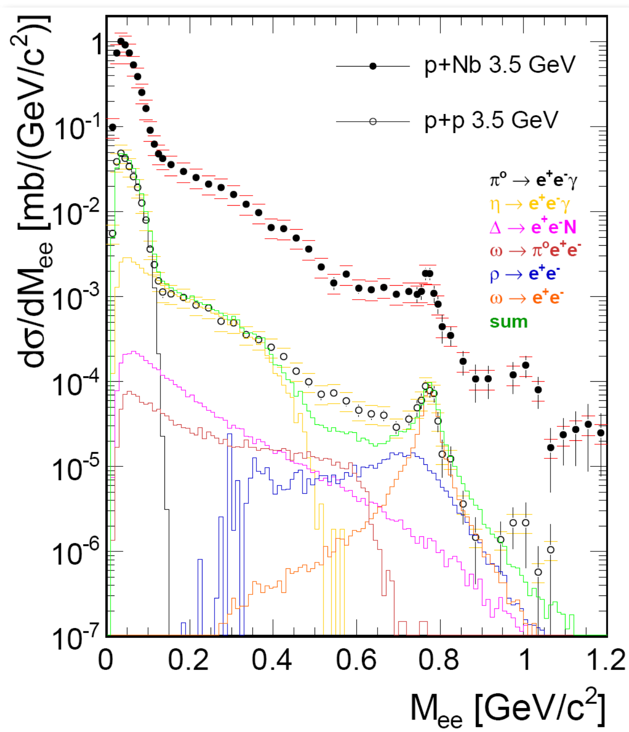

HADES, PLB 715 (2012)

- Broadening and/or mass shift?

HADES

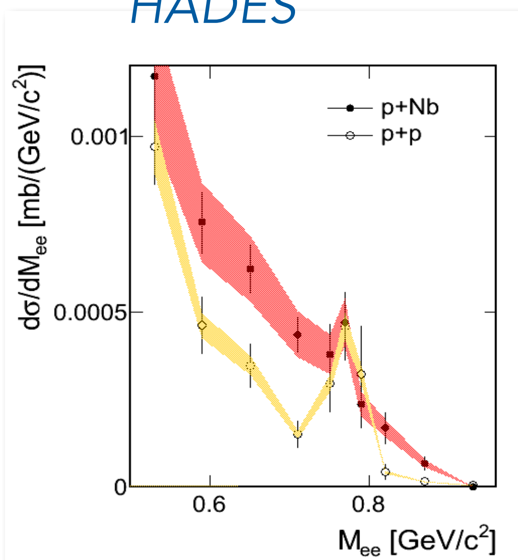

KEK-PS E325

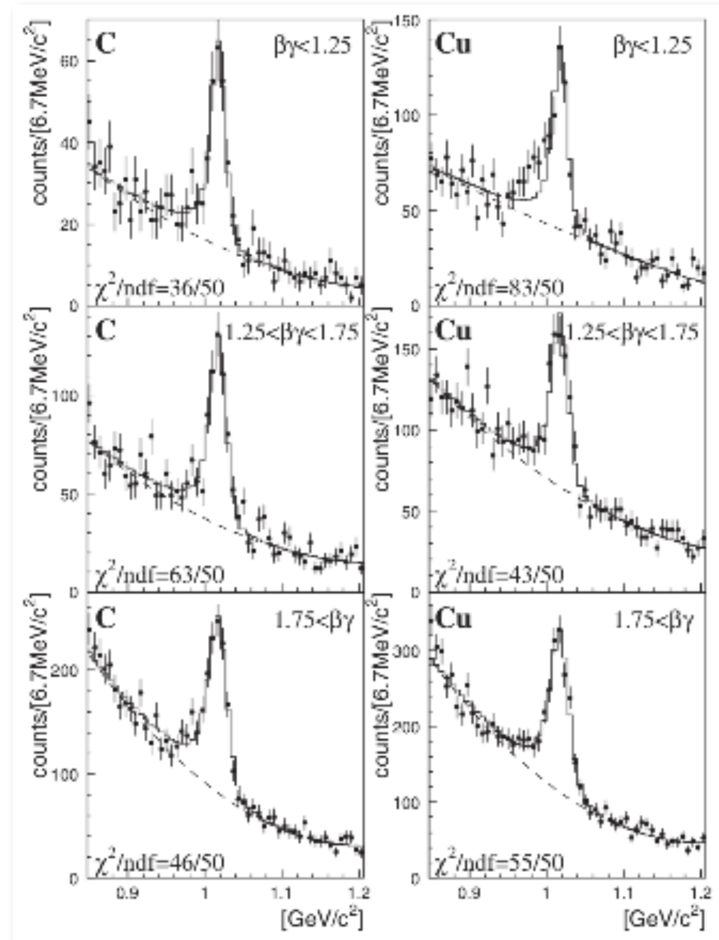

KEK-PS E325, PRL 98, 042501 (2007)

The existing and upcoming high-μ_b experiments

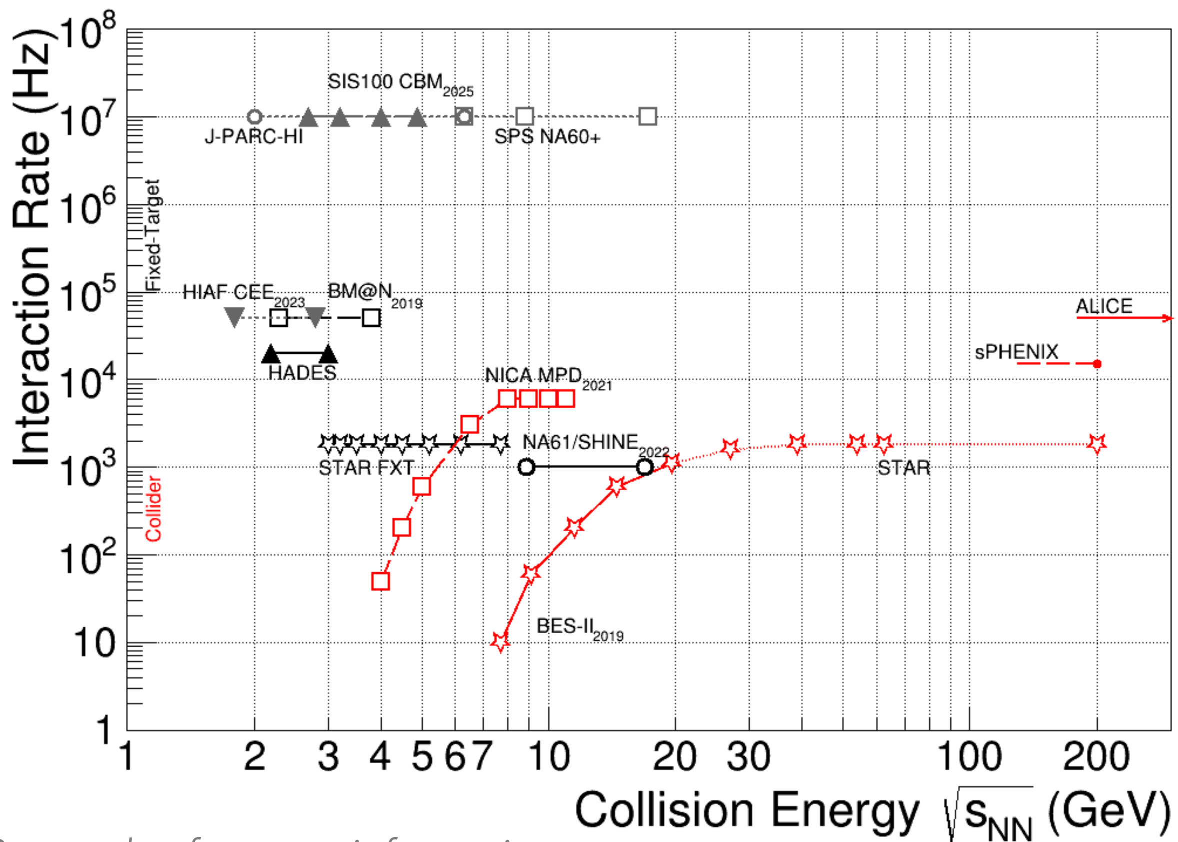

T. Galatyuk, QM2018, see also for more information

Current facilities for high μ_B physics

NA61 – SPS

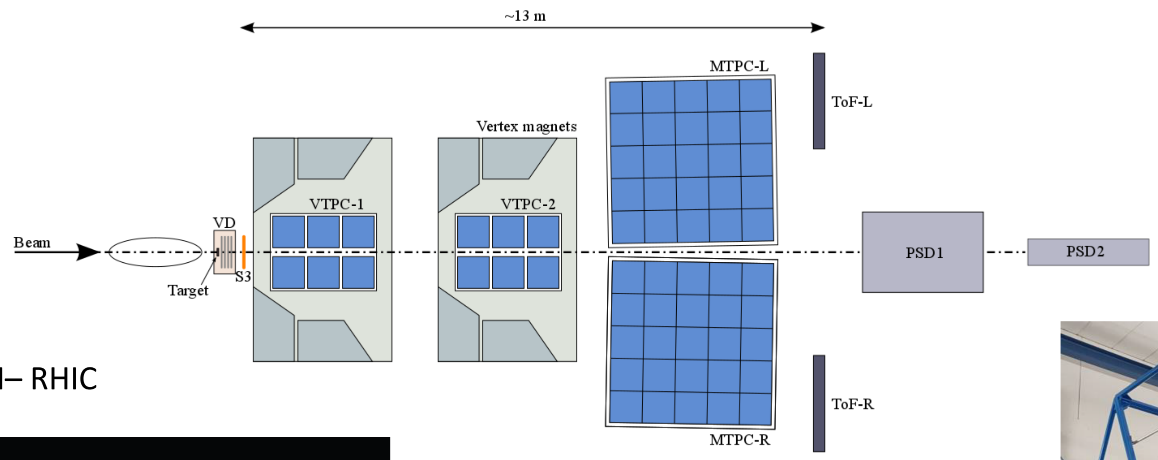

STAR-*BES*II– RHIC

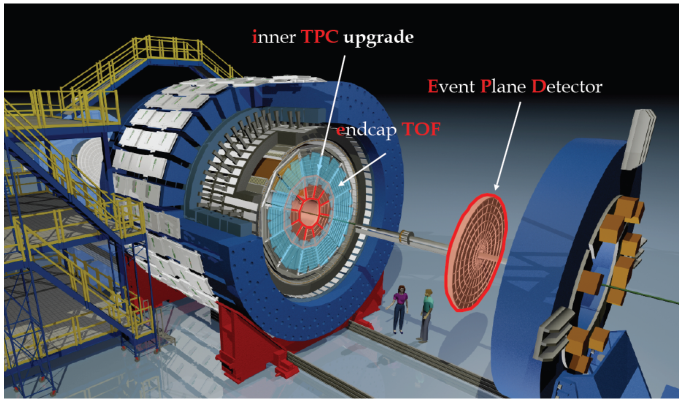

HADES – FAIR

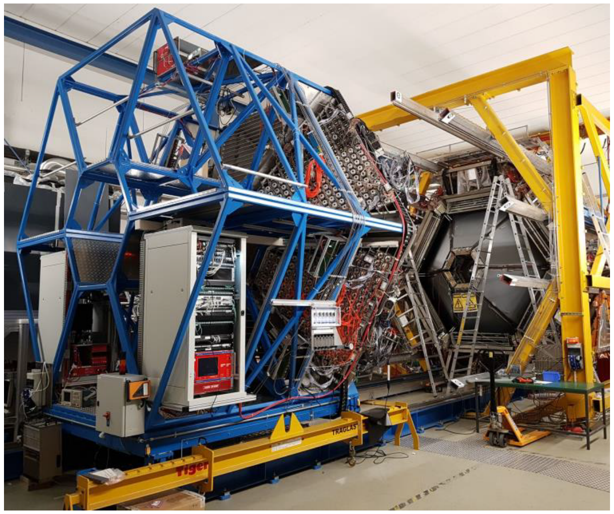

Future facilities for high μ_B physics

NA60^{+} – SPS

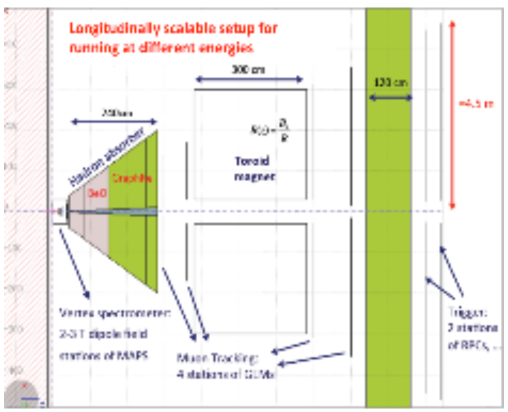

MPD – NICA

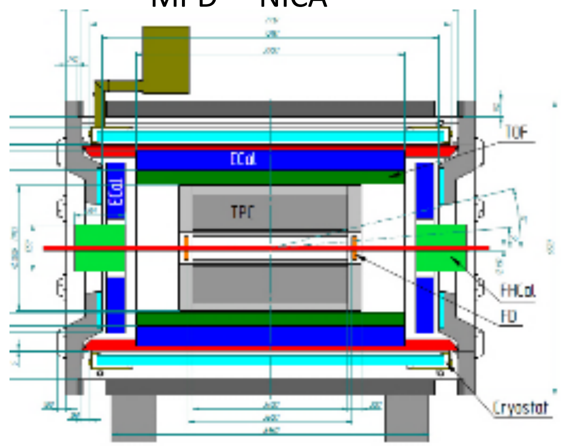

CBM– FAIR

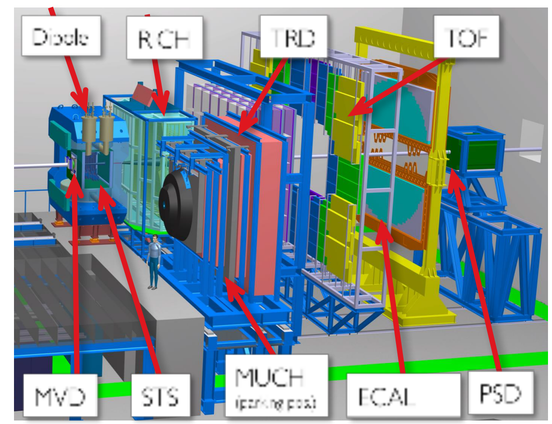

DHS – JPARC-HI

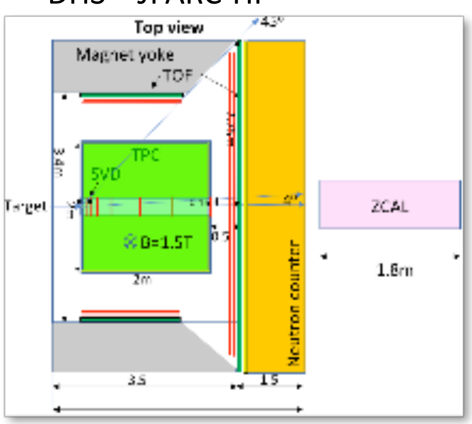

BM@N – NICA

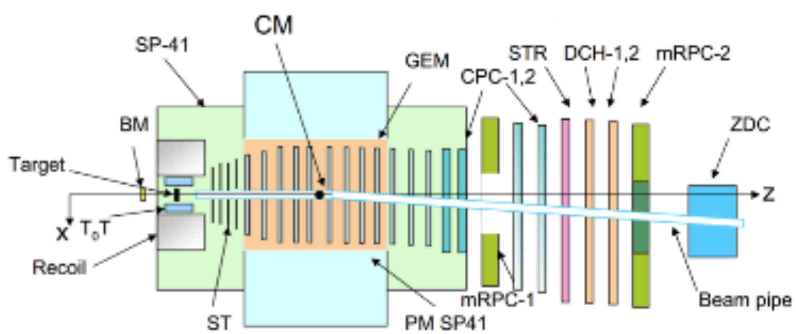

CEE– HIAF

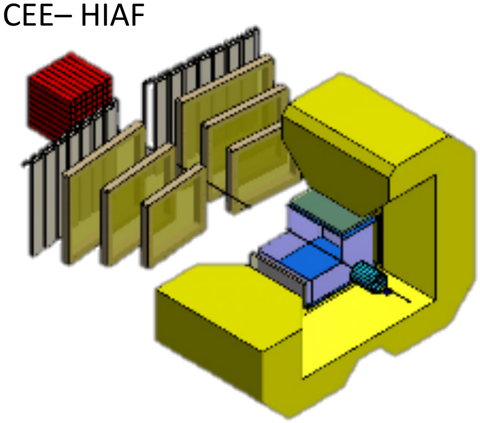

Hadron physics facilities with in-medium program

PANDA– *FAIR*

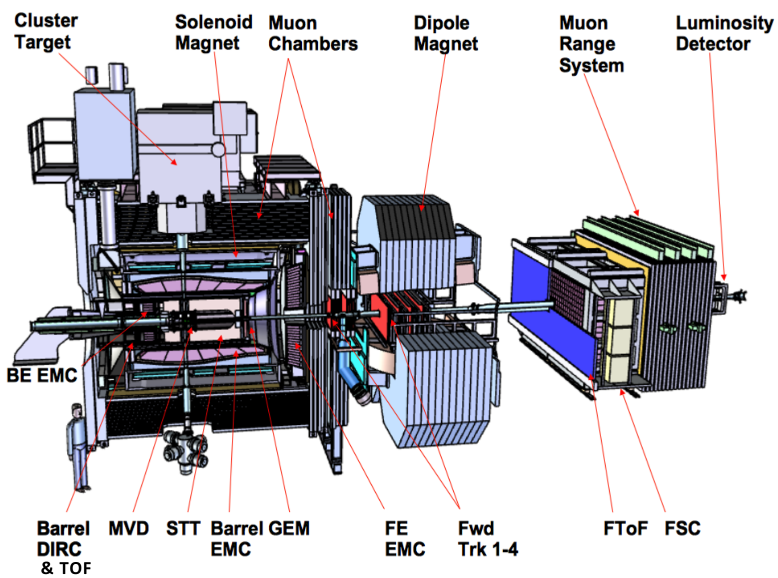

CLAS12– *JLAB*

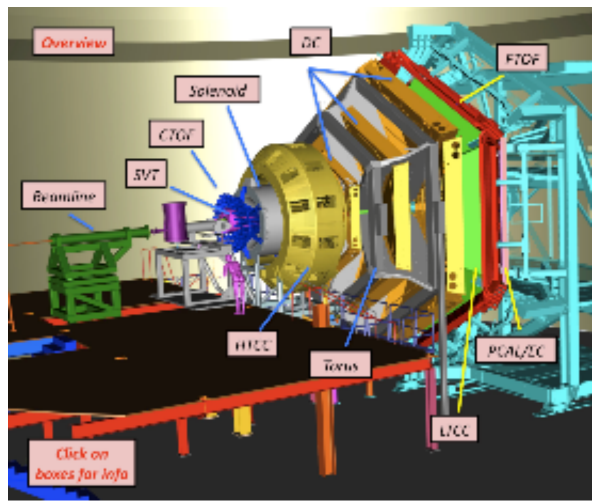

E16 – *J* PARC

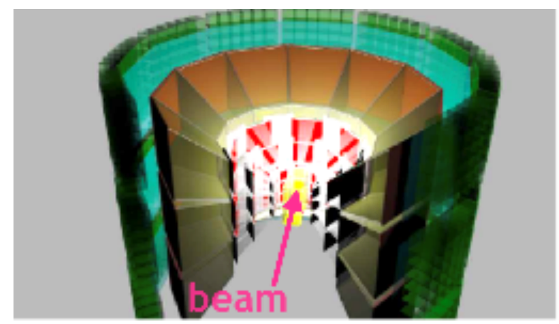

Summary

- Increasing effort world-wide to explore the high-μ_B region of the QCD phase diagram with state-of-the-art detectors.
- Vector mesons valuable probe to monitor the properties of dense matter
- Strong modification due to meson-baryon coupling
- Thermal rates can be used as “standard candle” to explore phase space “trajectories”
- Possible link to chiral symmetry restoration through $a_1 - \rho$ mixing
- “Sub-threshold” production of multi-strange baryons not understood at high-μ_B
- No (OZI) anomalous suppression of ϕ in-medium (cold matter) cross section
- Further experimental progress depends on high-statistics data for cold-matter and hot & dense matter studies

Yet another potential phase of QCD matter

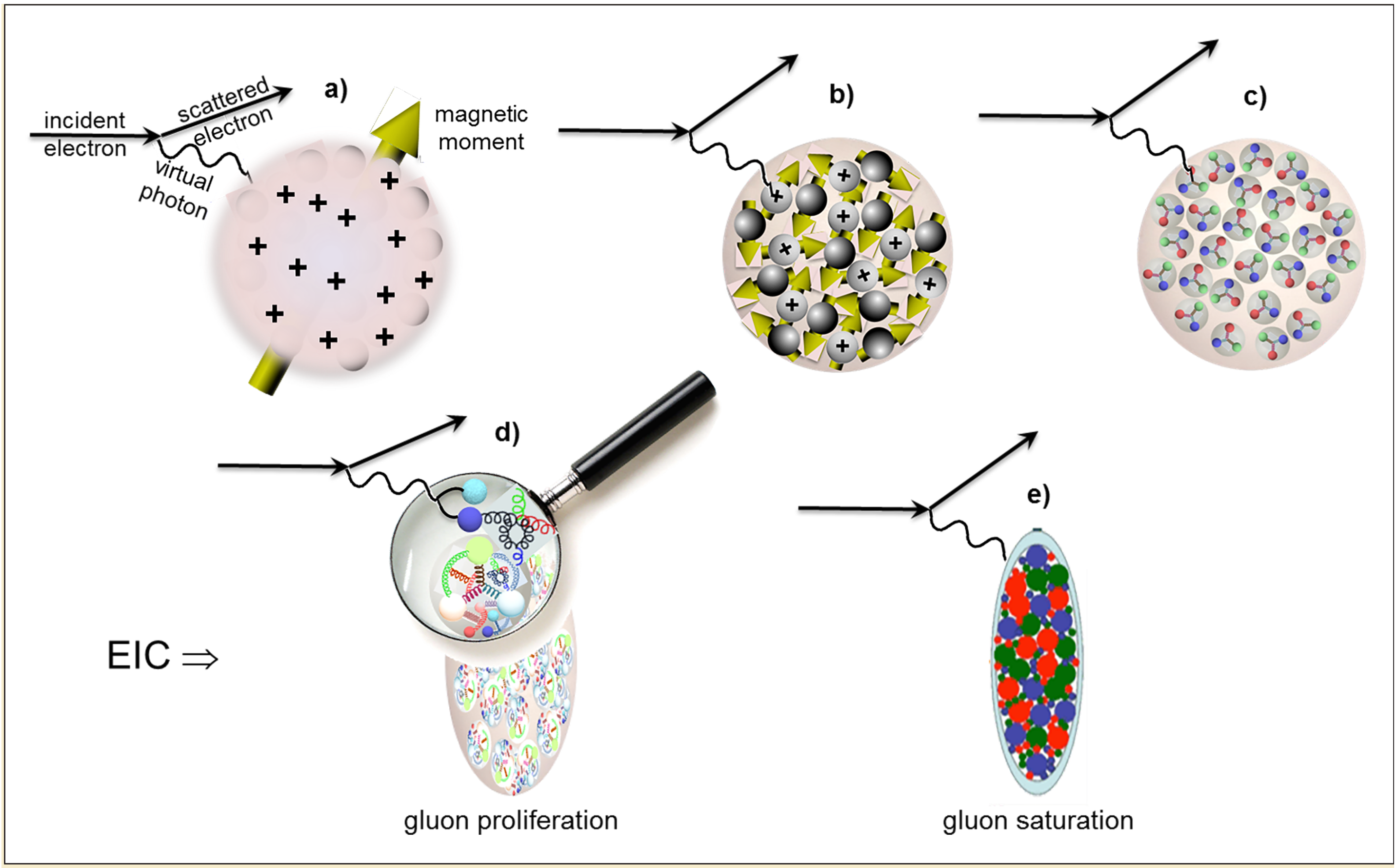

QCD Matter at Extreme Gluon Density

What happens to the gluon density in nuclei at high energy? Does it saturate, giving rise to a gluonic matter component of universal properties in all nuclei, even the proton? How does the nuclear environment affect quark and gluon distributions and interactions inside nuclei? Do the abundant low-momentum gluons remain confined within nucleons inside nuclei?

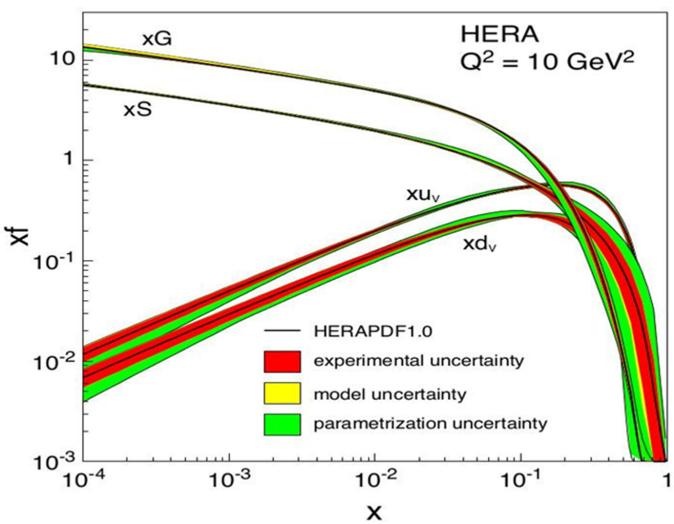

FIGURE 2.8 A global fit to parton distribution functions of the proton based on deep inelastic scattering data obtained at the Hadron-Electron Ring Accelerator (HERA). Distribution of gluons, G, sea quarks, S, and valence up and down quarks, u_v and d_v, are shown as a function of Bjorken *x*. SOURCE: Adapted from H. Abramowicz et al., 2015, Combination of measurements of inclusive deep inelastic $e^{\pm}p$ scattering cross sections and QCD analysis of HERA data, *Eur. Phys. J.* C75:580.

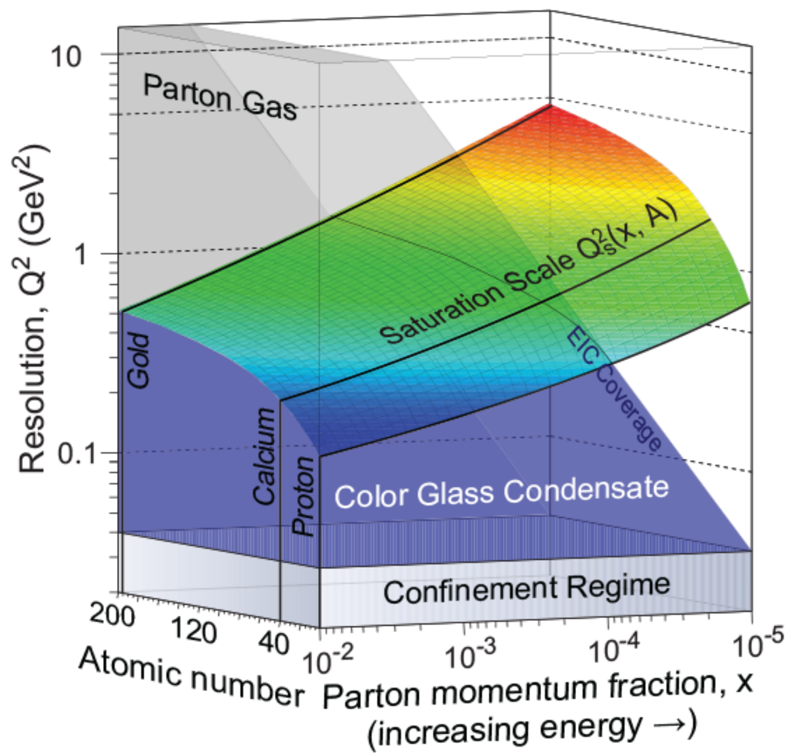

***Figure 2.18:** The schematic QCD landscape in probe resolving power (increasing upward) vs. energy (increasing toward the right), as a function of the atomic number of the nucleus probed. Electron collisions with heavy nuclei at the EIC will map the predicted saturation surface (colored surface) with the CGC region below that surface. Spatial distributions extracted from exclusive reactions (see text) will help demarcate the CGC region from the confinement regime.*

Machine to study this Physics: Electron – heavy ion collider

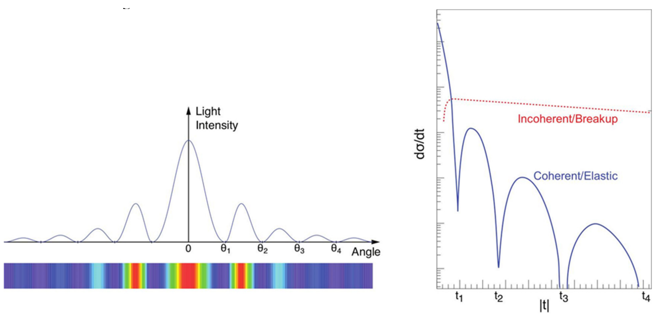

FIGURE 2.9 *Left*: Diffraction pattern in optics, showing the light intensity landing on a screen behind a circular obstacle. *Right*: The expected differential cross section for coherent and incoherent diffractive production of J/ψ particles on nuclei. The variable *t* is related to the momentum carried by the virtual photon, which is a measure of the scattering angle. The incoherent/breakup curve is explained in the text. SOURCE: *Reaching for the Horizon*, 2015 DOE/NSF Long Range Plan for U.S. Nuclear Science.

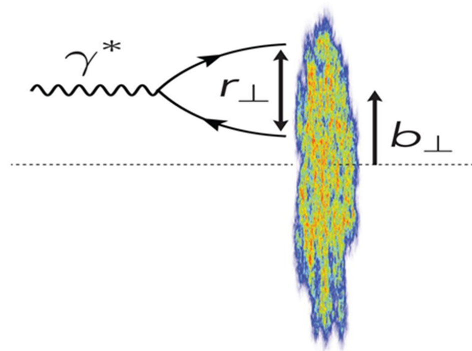

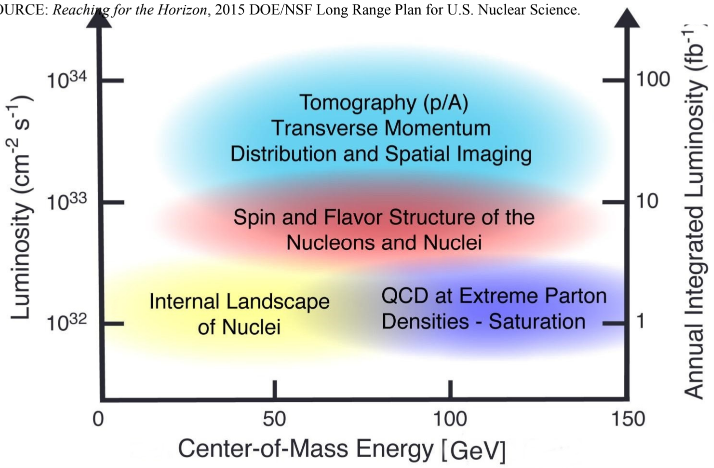

FIGURE 2.4 The energy-luminosity landscape that encapsulates the physics program of an Electron-Ion Collider. The horizontal axis shows the center-of-mass energy of the collider when operated in electron-proton mode. The two vertical axes show the instantaneous and annual integrated (electron-nucleon) luminosity; the latter is in units of inverse femtobarns, and assumes a running time of 10^7 seconds per year. SOURCE: Presentation of EIC Science by A. Deshpande on behalf of the EIC Users Group

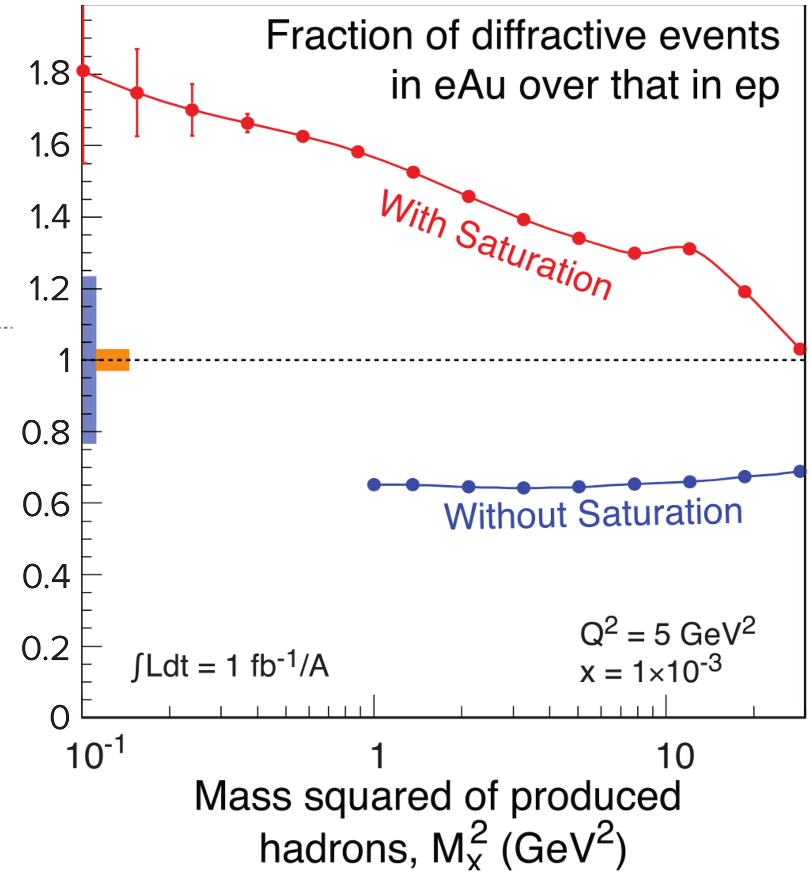

Figure 2.19: *The ratio of diffractive over total cross section for DIS on a gold nucleus normalized to DIS on a proton, for different values of the mass-squared of hadrons produced in the collisions, predicted with (red curve) and without (blue curve) gluon saturation. The projected experimental uncertainties are smaller than the plotted points while the range of each model's prediction (shaded bands on the left side) is smaller than the difference caused by saturation.*

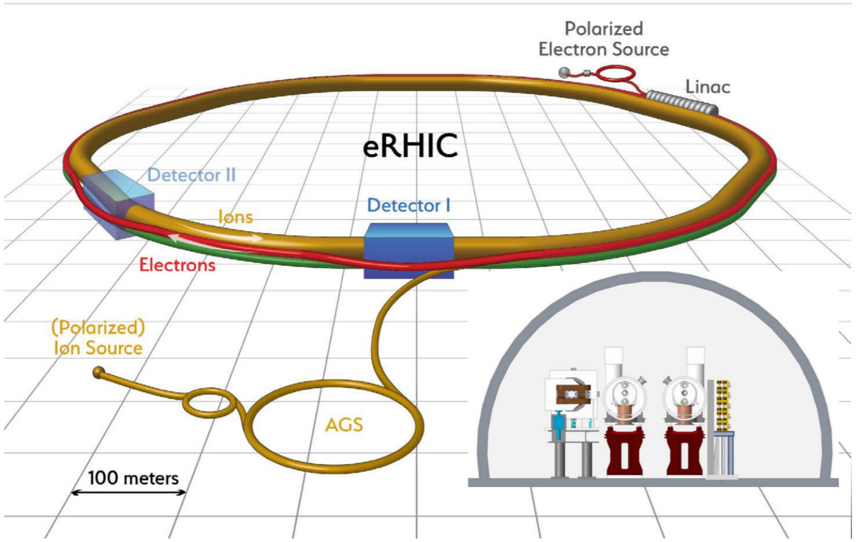

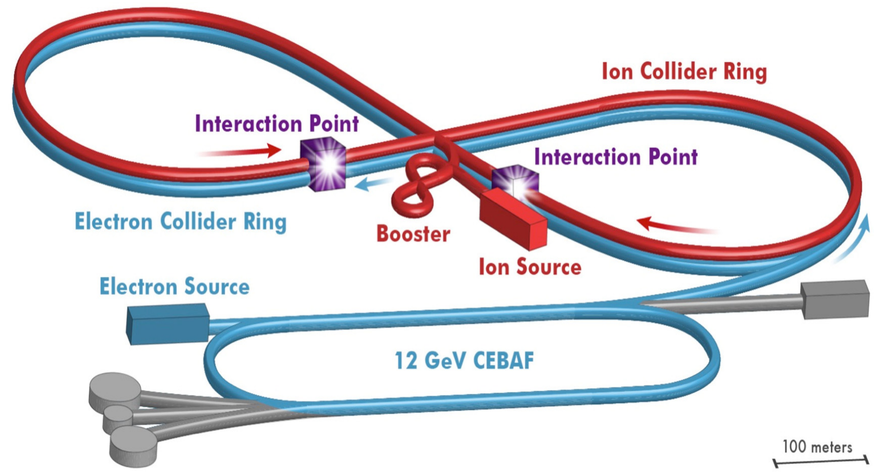

FIGURE 4.4 Schematic layout of the Jefferson Laboratory Electron Ion Collider design. SOURCE: Thomas Jefferson National Accelerator Facility.

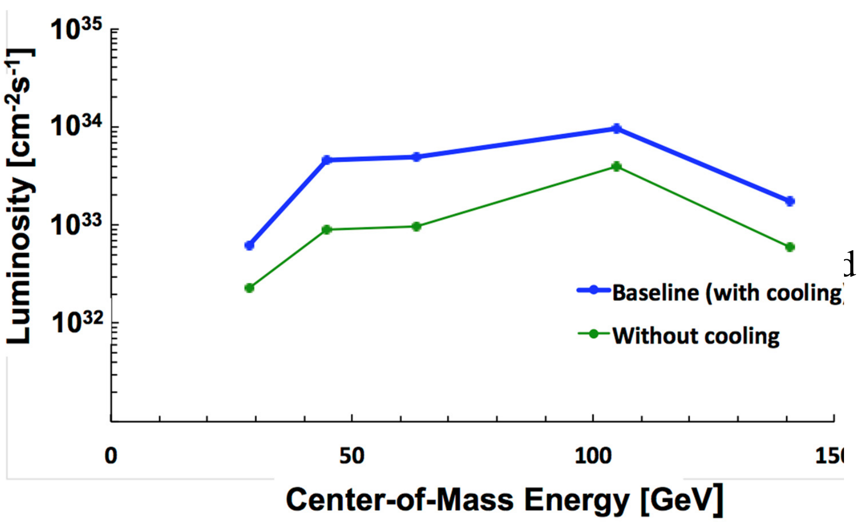

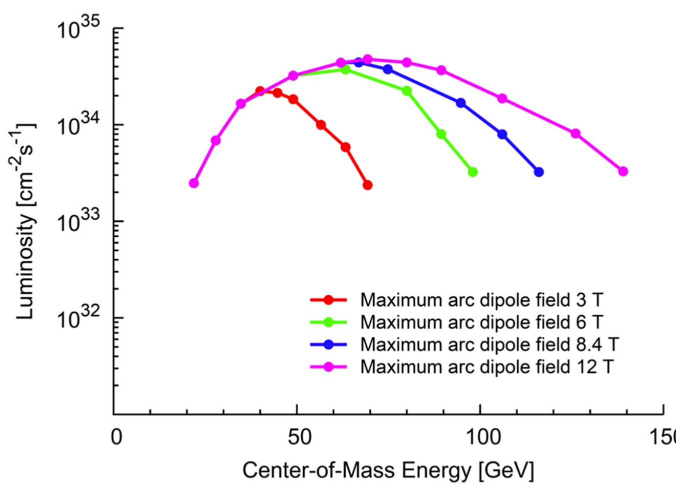

Jefferson Laboratory Electron Ion Collider (JLEIC) e-p luminosity as a function of center- of-mass energy with the 3 T hadron arc magnets currently under development (red curve and the parameter sets in Table 4.2). The other curves show the potential of magnets with still higher fields. SOURCE: Y. Zhang, 2017, "Progress in JLEIC Design," EIC Accelerator Collaboration Meeting, Brookhaven National Laboratory, October 2017.